TECHNICAL REPORT CERC-87-17

CHARACTERISTICS OF REEF BREAKWATERS

by

John P. Ahrens

Coastal Engineering Research Center

DEPARTMENT OF THE ARMY
Waterways Experiment Station, Corps of Engineers
PO Box 631, Vicksburg, Mississippi 39180-0631

December 1987
Final Report

Approved For Public Release; Distribution Unlimited

US Army Corps
of Engineers

Unclassified

SECURITY CLASSIFICATION OF THIS PAGE

REPORT DOCUMENTATION PAGE

Form Approved
OMB No 0704-0188
Exp. Date Jun 30, 1986

1a. REPORT SECURITY CLASSIFICATION Unclassified		1b. RESTRICTIVE MARKINGS			
2a. SECURITY CLASSIFICATION AUTHORITY		3. DISTRIBUTION/AVAILABILITY OF REPORT Approved for public release; distribution unlimited.			
2b. DECLASSIFICATION/DOWNGRADING SCHEDULE					
4. PERFORMING ORGANIZATION REPORT NUMBER(S) Technical Report CERC-87-17		5. MONITORING ORGANIZATION REPORT NUMBER(S)			
6a. NAME OF PERFORMING ORGANIZATION USAEWES, Coastal Engineering Research Center	6b. OFFICE SYMBOL (If applicable)	7a. NAME OF MONITORING ORGANIZATION			
6c. ADDRESS (City, State, and ZIP Code) PO Box 631 Vicksburg, MS 39180-0631		7b. ADDRESS (City, State, and ZIP Code)			
8a. NAME OF FUNDING/SPONSORING ORGANIZATION US Army Corps of Engineers	8b. OFFICE SYMBOL (If applicable)	9. PROCUREMENT INSTRUMENT IDENTIFICATION NUMBER			
8c. ADDRESS (City, State, and ZIP Code) Washington, DC 20314-1000		10. SOURCE OF FUNDING NUMBERS			
		PROGRAM ELEMENT NO.	PROJECT NO.	TASK NO	WORK UNIT ACCESSION NO 31616

11. TITLE (Include Security Classification)

Characteristics of Reef Breakwaters

12. PERSONAL AUTHOR(S)
Ahrens, John P.

13a. TYPE OF REPORT Final report	13b. TIME COVERED FROM _____ TO _____	14. DATE OF REPORT (Year, Month, Day) December 1987	15. PAGE COUNT 62

16. SUPPLEMENTARY NOTATION
Available from National Technical Information Service, 5285 Port Royal Road, Springfield, VA 22161.

17.	COSATI CODES		18. SUBJECT TERMS (Continue on reverse if necessary and identify by block number)
FIELD	GROUP	SUB-GROUP	Breakwaters (LC)
			Water waves (LC)

19. ABSTRACT (Continue on reverse if necessary and identify by block number)

A laboratory study was conducted to determine the stability, wave transmission, wave reflection, and energy dissipation characteristics of reef breakwaters. Reef breakwaters are low-crested structures comprised of a homogeneous pile of stone with individual stone weights in the range of those ordinarily used in the armor and first underlayer of traditional multilayered breakwaters. The study included over two hundred tests, all using irregular wave conditions.

Results of the study are discussed and summarized through the use of equations fit to the data. The equations fit the data well, are consistent with the physics of the various phenomena as they are currently understood, and approach logical limiting values.

(Continued)

20. DISTRIBUTION/AVAILABILITY OF ABSTRACT ☒ UNCLASSIFIED/UNLIMITED ☐ SAME AS RPT ☐ DTIC USERS	21. ABSTRACT SECURITY CLASSIFICATION Unclassified	
22a. NAME OF RESPONSIBLE INDIVIDUAL	22b. TELEPHONE (Include Area Code)	22c. OFFICE SYMBOL

DD FORM 1473, 84 MAR

83 APR edition may be used until exhausted
All other editions are obsolete

SECURITY CLASSIFICATION OF THIS PAGE
Unclassified

19. ABSTRACT (Continued).

Important findings include:

a. A reef stability model which can predict the degree of degration of the struc-
ture as a function of severity of irregular wave attack.

b. A wave transmission model capable of predicting the amount of wave energy
transmitted over and through the structure for both submerged and nonsubmerged
reefs.

c. A wave reflection model which makes accurate predictions of energy reflected
from the reef for a wide range of wave conditions and structure heights.

d. A model which predicts the amount of incident wave energy dissipated by the
reef.

PREFACE

CONTENTS

CHARACTERISTICS OF REEF BREAKWATERS

PART I: INTRODUCTION

1. A reef breakwater is a low-crested rubble-mound breakwater without the traditional multilayer cross section. This type of breakwater is little more than a homogeneous pile of stones with individual stone weights similar to those ordinarily used in the armor and first underlayer of conventional breakwaters.

2. In recent years a number of low-crested breakwaters have been built or considered for use at a variety of locations. Most of these structures are intended to protect a beach or reduce the cost of beach maintenance. Other applications include protecting water intakes for power plants and entrance channels for small-boat harbors and providing an alternative to revetment for stabilizing an eroding shoreline. In situations where only partial attenuation of waves on the leeside of a structure is required, or possibly even advantageous, a low-crested rubble-mound breakwater is a logical selection. Since the cost of a rubble-mound breakwater increases rapidly with the height of the crest, the economic advantage of a low-crested structure over a traditional breakwater that is infrequently overtopped is obvious. Because the reef breakwater represents the ultimate in design simplicity, it could be the optimum structure for many situations. Unfortunately, the performance of low-crested rubble-mound structures, particularly reef breakwaters, is not well documented or understood.

Background

3. A number of papers have noted that armor on the landside slope of a low-crested breakwater is more likely to be displayed by heavy overtopping than armor on the seaward face (Lording and Scott 1971, Raichlen 1972, and Lillevang 1977). Raichlen discusses the characteristics of overtopping over the crest and the inherent complexity of the problem. Walker, Palmer, and Dunham (1975) give a carefully reasoned discussion of the many factors influencing stability of heavily overtopped rubble-mound breakwaters. They also show a figure which suggests what armor weight is required for stability

3

on the backside of a low-crested breakwater. Unfortunately, the data scatter shown in the figure undermines confidence in the suggested armor weights.

4.   In Australia, the breakwater at Rosslyn Bay was damaged severely during Cyclone David in 1976 (Bremner et al. 1980). The crest height of the structure was reduced as much as 4 m but still functioned effectively as a submerged breakwater for over 2 years until it was repaired. Based on the surprisingly good performance of the damaged Rosslyn Bay breakwater and the findings from model tests, a low-crested design was chosen for the breakwater at Townsville Harbor, Australia. This breakwater is unusual because it was built entirely of stone in the 3- to 5-ton* range (Bremner et al. 1980). Reef breakwaters, as described in this paper, are very similar to the Townsville breakwater except a wider gradation of stone was used in the model breakwater tests discussed herein.

5.   Seelig (1979) conducted an extensive series of model tests to determine wave transmission and reflection characteristics of low-crested breakwaters, including submerged structures. From these tests Seelig concluded that the component of transmission resulting from wave overtopping was very strongly dependent on the relative freeboard (i.e., freeboard divided by incident significant wave height). Recent work by Allsop (1983) with multilayered, low-crested breakwaters shows that wave transmission is strongly dependent on a dimensionless freeboard parameter which includes the zero-crossing period of irregular wave conditions. Allsop did not find substantial wave period dependency in his evaluation of breakwater stability. He indicates, however, that since wave transmission (which largely results from overtopping) is dependent on period, then possible stability of the backside slope would also be a function of wave period.

Scope

6.   A study currently being conducted at the US Army Engineer Waterways Experiment Station's Coastal Engineering Research Center is intended to document the performance of low-crested breakwaters. This paper discusses laboratory model tests of reef breakwaters and provides information on their stability to wave attack, wave transmission and reflection characteristics, and wave energy dissipation.

---

* Metric ton.

7.   To date, 205 two-dimensional laboratory tests of reef breakwaters have been completed. These tests were conducted in a 61-cm-wide channel within CERC's 1.2- by 4.6- by 42.7-m tank (Figure 1). All tests were
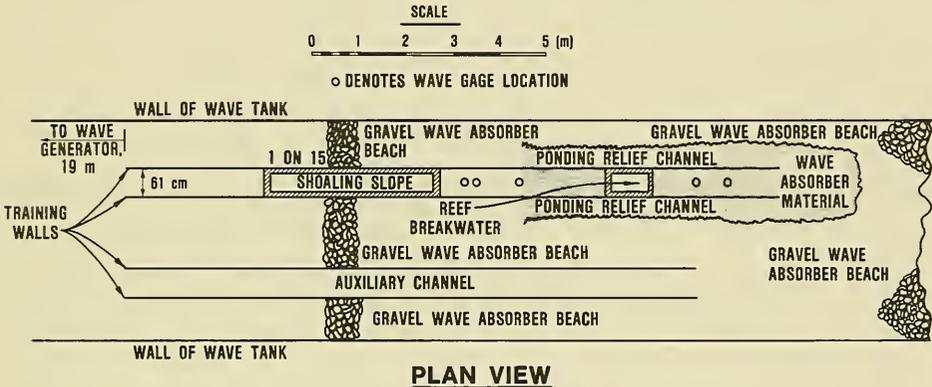
PLAN VIEW

Figure 1. Plan view of wave tank and test setup

conducted with irregular waves. The spectra used had wave periods of peak energy density T_p* ranging from about 1.45 to 3.60 sec, and water depth at the structure d_s ranged from 25 to 30 cm. Signals to control the wave blade were stored on magnetic tape and transferred to the wave generator through a computer data acquisition system (DAS). For this study four files were stored on the tape which could produce a spectrum with a distinct period of peak energy density. Table 1 gives the nominal period of peak energy density for each file.

8.   If there were no attenuation of the signal to the wave generator, the files used were intended to produce a saturated spectrum at all frequences above the frequency of peak energy density for the water depth at the wave blade. For frequencies lower than those of the peak, the energy density decreased rapidly. This procedure produced a spectrum of the Kitaigorodskii type as described by Vincent (1981). The amplitude of the signal to the wave generator was attenuated by a 10-turn potentiometer in a voltage divider

---

*   For convenience, symbols and unusual abbreviations are listed and defined in the Notation (Appendix C).

5

Table 1

Period of Peak Energy Density

for Each Tape File

Tape File	Approximate T_p , sec
1	1.45
2	2.25
3	2.86
4	3.60

network which allowed control of the wave heights generated. In addition, the waves were generated in a water depth 25 cm greater than at the breakwater and shoaled to the water depth at the structure over a 1-V on 15-H slope (see Figure 2). This setup ensures that severe conditions can be developed at the
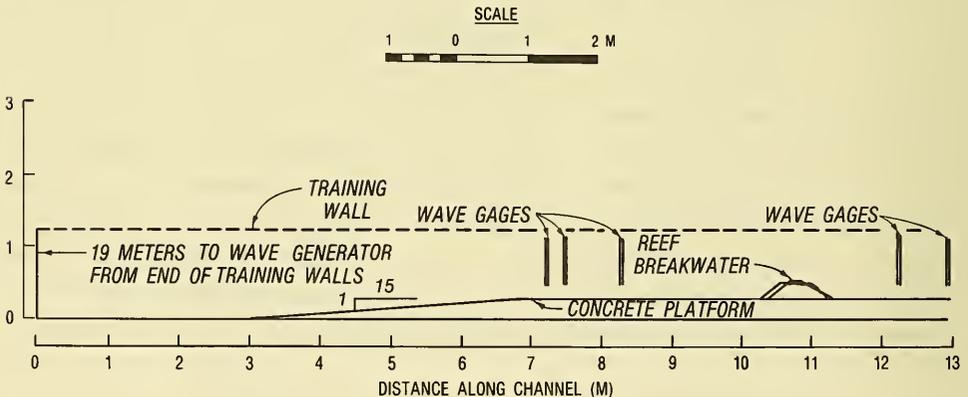
Figure 2. Cross section of test channel

structure site. Incident zero-moment wave heights H_{mo} ranged from about 1 to 18 cm.

9. Three parallel wire-resistance wave gages were used in front of the breakwater to resolve the incident and reflected wave spectra using the method of Goda and Suzuki (1976), and two wave gages were placed behind the structure to measure the transmitted wave height. The location of gages is shown in Figure 2. During data collection gages were sampled at a rate of 16 times per second for 256 sec by the same DAS which controlled the wave generator motion.

6

10. Two types of model tests were conducted during this study: stability and previous damage tests. Each type followed a prescribed sequence.

Stability Tests

11. For a stability test the following test sequence was used:

a. Rebuild the breakwater from the previously damaged condition.

b. Survey the breakwater to document its initial condition.

c. Calibrate the wave gages.

d. Select the tape file and signal attenuation setting.

e. Start the wave generator and run waves.

f. Collect wave data (several or more times).

g. Stop the wave generator.

h. Survey the breakwater to document its final condition.

The duration of wave action was from 1-1/2 hr for a test using the File 1 spectrum to 3-1/2 hr for a File 4 spectrum. Generally, the technicians observing the tests thought that most of the stone movement occurred during the first 10 or 15 min of wave generation, so the final survey is regarded as an equilibrium profile for the structure. In rebuilding the breakwater the technicians rarely touched the stone but merely pushed it around by foot until the shape conformed to the desired initial profile. This procedure was a conscious effort to avoid overly careful placement of the stone. Outlines of the desired initial profile were fixed to the walls of the testing channel, and a moveable template was used to ensure that the initial profile was reasonably close to the desired profile. Initial configuration of the breakwater for a stability test was a narrow, trapezoidal shape with seaward and landward slopes of 1V on 1.5H (Figure 3). Crest widths were three typical stone dimensions wide, using the cube root of the volume of the median weight stone W_{50} as the typical dimension d_{50} . Figure 3 also shows a typical profile after moderately severe wave attack during a stability test. Wave transmission and reflection also were measured during a stability test.
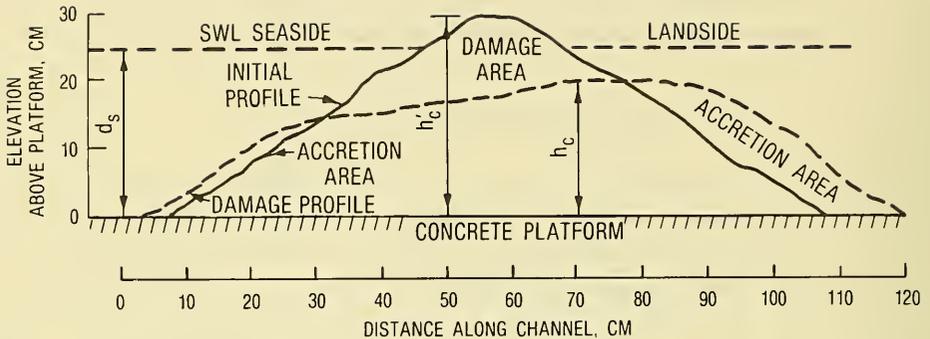
Figure 3. Cross-sectional view of initial and typical damaged reef profiles
(swl denotes still-water level)

Previous Damage Tests

12. Previous damage tests were conducted to answer the question of how
the breakwater would perform for moderate wave conditions after it had been
damaged by very severe wave conditions. For previous damage tests there was
very little readjustment of the damage profile from test to test; conse-
quently, the breakwater was not rebuilt at the end of a test. No stability
information was obtained from these tests, and the duration of wave action was
only half an hour; however, wave transmission and reflection were measured.
Previous damage tests were performed in the following sequence:

> a. Survey breakwater for last test which becomes initial survey
>   for current test.
>
> b. Calibrate wave gages.
>
> c. Select wave file and signal attenuation setting.
>
> d. Start generator and run waves for half an hour.
>
> e. Collect wave data (two or three times).
>
> f. Stop wave generator.
>
> g. Survey breakwater as noted above in Step 1.

13. All 205 of the completed tests of this study can be divided logi-
cally into 10 subsets or test series. Because of the test plan, stability
test series have odd numbers, and previous damage test series have even num-
bers. Table 2 lists the basic information about each subset.

14. Two different sizes of stone were used during this study. For sub-
sets 1 through 6 an angular quartzite with a median weight of 17 g was used,

8

Table 2

Basic Data for Each Subset

Subset No.	No. of Tests	Water Depth d_s , cm	Crest Height "as built" h_c' , cm	Median Stone Weight W_{50} , g	Area of Breakwater Cross Section A_t , cm^2
1	27	25	25	17	1,170
2	3	25	NA*	17	1,170
3	29	25	30	17	1,560
4	12	25	NA	17	1,560
5	41	25	35	17	2,190
6	11	25	NA	17	2,190
7	38	25	32	71	1,900
8	26	25	NA	71	1,900
9	13	30	32	71	1,900
10	5	30	NA	71	1,900

* NA denotes not applicable to previous damage test series.

and for subsets 7 through 10 a blocky to angular diorite with a median weight of 71 g was used. Photo 1 depicts the stone, and Table 3 summarizes information about it.

Table 3

Stone and Gradation Characteristics

Characteristic	Quartzite	Diorite
2% weight (g)	7.0	14.0
Median weight, W_{50} (g)	17.0	71.0
98% weight (g)	28.0	139.0
Density (g/cm^3)	2.63	2.83
Porosity (%)	45	44

Profile Surveys

15. Initial and final profiles of the reef were obtained by survey.
The survey rods had feet attached with ball-and-socket connectors. For the
small stone used for subsets 1 through 6, the foot of the survey rod had a
diameter of 2.54 cm; and for the somewhat larger stone used in subsets 7
through 10, the foot of the survey rod had a diameter of 3.81 cm. Three pro-
files were used to establish an average profile for the reef. One profile
line was exactly in the center of the wave channel, and the other two profile
lines were 15 cm on either side of center. The survey interval along the
channel was 3.05 cm.

PART III: STABILITY AND PERFORMANCE RESULTS

16.   The report herein consolidates findings from all of the data sub-
sets identified in Table 2 into general conclusions about the stability and
performance characteristics of reef breakwaters.   Specific characteristics in-
clude the stability of reef breakwaters to irregular wave attack, wave trans-
mission over and through the breakwater, wave reflection from the breakwater,
and dissipation of wave energy.   A mathematical model is developed for each
characteristic which provides a simple method to summarize findings from this
study and a convenient way to furnish results to potential users.   These math-
ematical models are intended to work together with the stability model fur-
nishing the equilibrium crest height to both transmission and reflection
models which together are used to estimate the amount of energy dissipated by
the reef.

Stability to Irregular Wave Attack

17.   The stability of reef breakwaters will be quantified by damage or
lack of damage during a test, the most important aspect of which is the reduc-
tion in crest height caused by wave attack.   This aspect of stability is
important because the performance of a reef breakwater will be judged largely
on its wave transmission characteristics.   Wave transmission is very sensitive
to crest height relative to water level.

Crest height reduction factor

18.   One of the most effective methods to evaluate damage to a reef
breakwater is to use the ratio of the crest height at the completion of a test
to the height at the beginning of the test before waves have been run.   This
ratio, h_c/h_c' , will be referred to as the crest height reduction factor.   For
comparing damage within a subset, h_c/h_c' is effective because it inherently
accounts for the random variation of one to two centimeters in the constructed
crest height from test to test within a subset.   Another advantage of the
crest height reduction factor is that all stability subsets have the same
natural limiting values of 1.0 and 0.0.

Stability number and
spectral stability number comparison

19.   Experience with the stability of traditional rubble-mound break-
waters to monochromatic waves suggests that one of the most important

11

variables to explain damage would be one similar to the stability number used by Hudson and Davidson (1975). The following definition is used for the stability number for tests with irregular waves:

$$N_s = \frac{H_{mo}}{\left(\dfrac{W_{50}}{w_r}\right)^{1/3} \left(\dfrac{w_r}{w_w} - 1\right)} \qquad (1)$$

where w_r is the density of stone and w_w is the density of water. Since these tests were conducted in fresh water, $w_w = 1.0$ g/cm^3. As far as the stability tests of reef breakwaters are concerned, it was apparent that tests with a higher period of peak energy density did more damage than similar tests with a smaller period of peak energy density. This finding is consistent with the results of a study conducted by Gravesen, Jensen, and Sorensen (1980) on the stability of high-crested, rubble-mound breakwaters exposed to irregular wave attack. According to the stability analysis of Gravesen, the spectral stability number is defined

$$N_s^* = \frac{\left(H_{mo}^2 \; L_p\right)^{1/3}}{\left(\dfrac{W_{50}}{w_r}\right)^{1/3} \left(\dfrac{w_r}{w_w} - 1\right)} \qquad (2)$$

where L_p is the Airy wave length calculated using T_p and the water depth at the toe of the reef d_s.

20. Figures 4 through 8 show comparisons of the effectiveness of the stability number and the spectral stability number in accounting for damage to reef breakwaters. In Figures 4, 5, 6, 7, and 8 the crest height reduction factor is plotted versus the traditional stability number and the spectral stability number for stability subsets 1, 3, 5, 7, and 9, respectively. The figures show that there is less scatter in the damage trends when they are plotted versus the spectral stability number. They also show that there is little or no damage for spectral stability numbers less than about six but that damage increases rapidly for spectral stability numbers above eight. In the following analysis the spectral stability number will be used to define
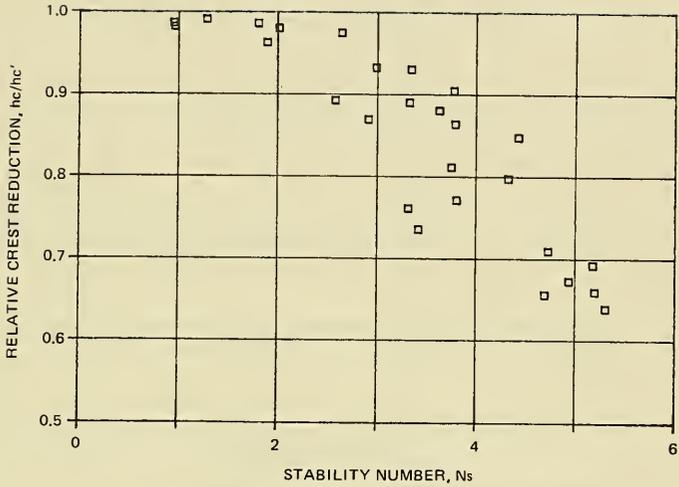
a. Crest height reduction factor versus the stability number
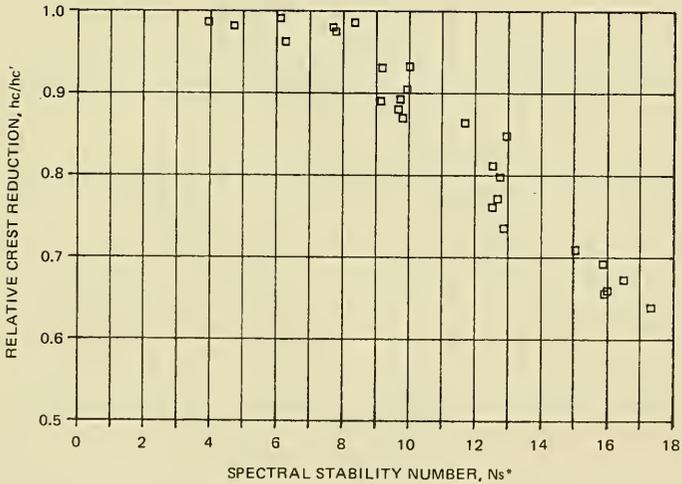
b. Crest height reduction factor versus the spectral stability number

Figure 4. Stability comparisons for subset 1
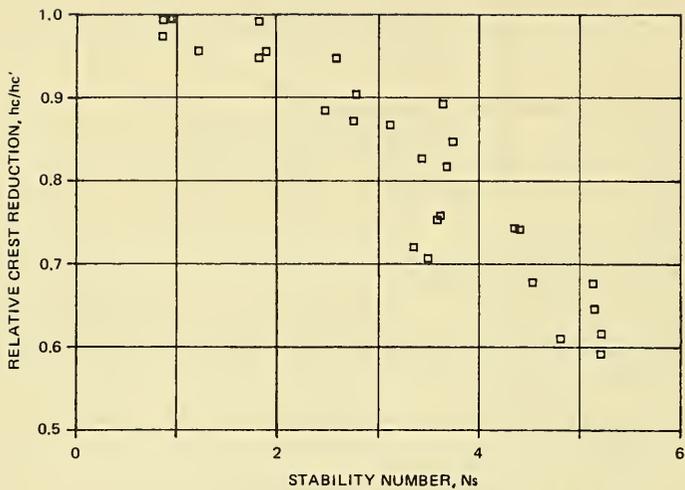
13

a. Crest height reduction factor versus the stability
number
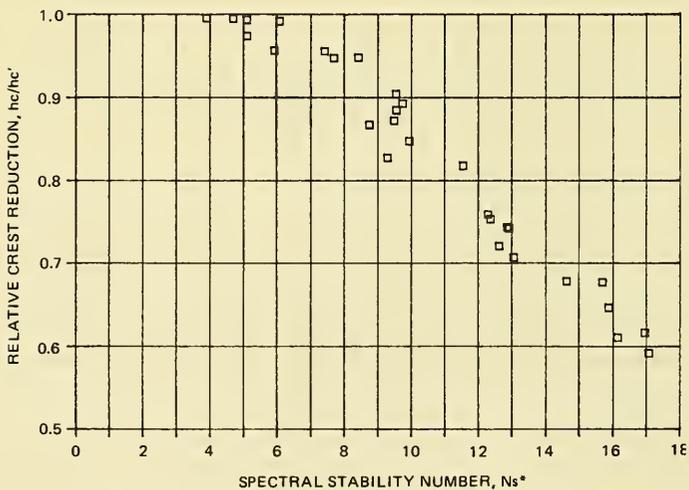
b. Crest height reduction factor versus the spectral
stability number

Figure 5. Stability comparisons for subset 3
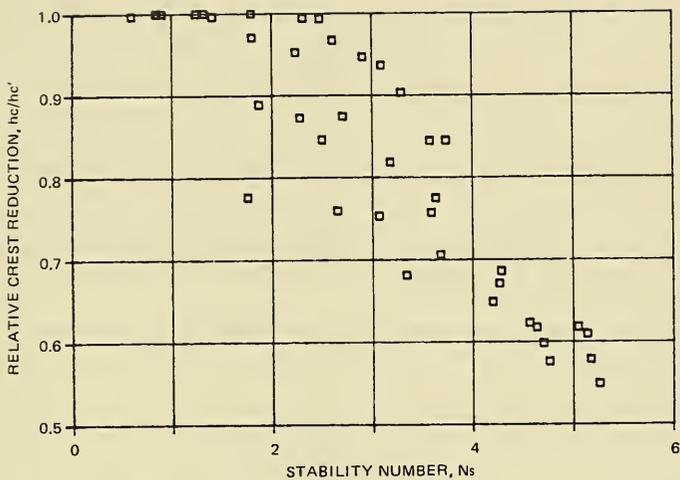
a. Crest height reduction factor versus the stability number
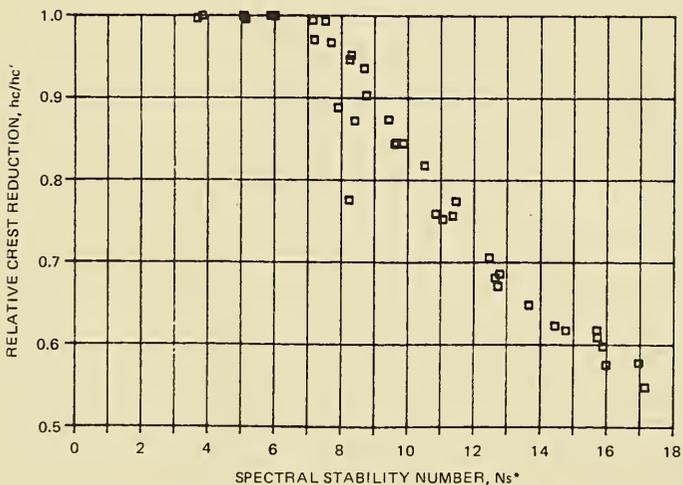
b. Crest height reduction factor versus the spectral stability number

Figure 6. Stability comparisons for subset 5
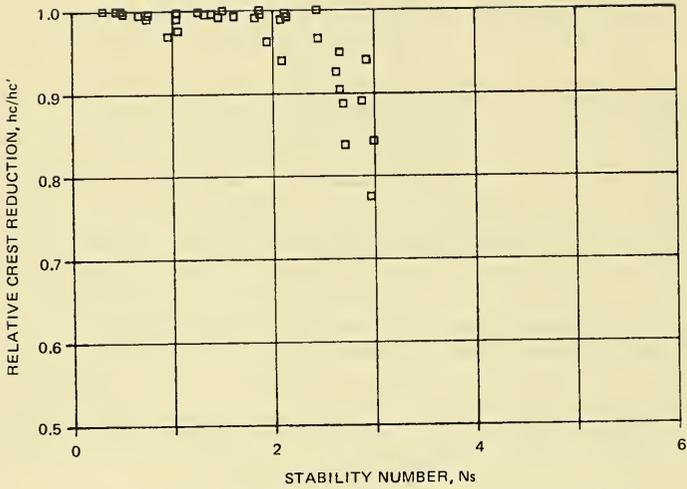
15

a. Crest height reduction factor versus the stability number
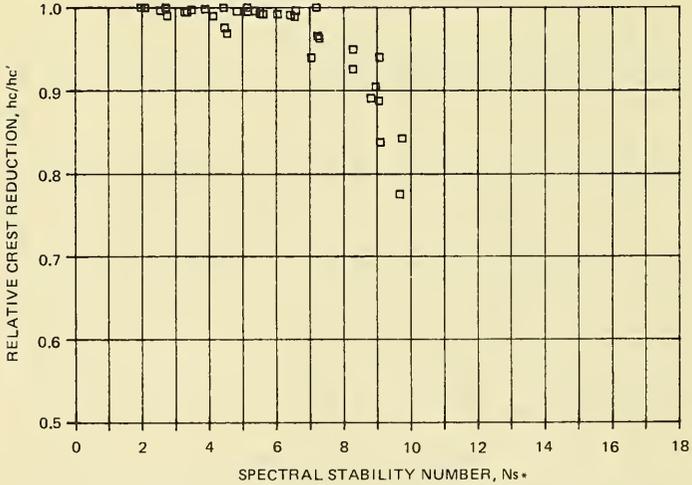
b. Crest height reduction factor versus the spectral stability number

Figure 7. Stability comparisons for subset 7
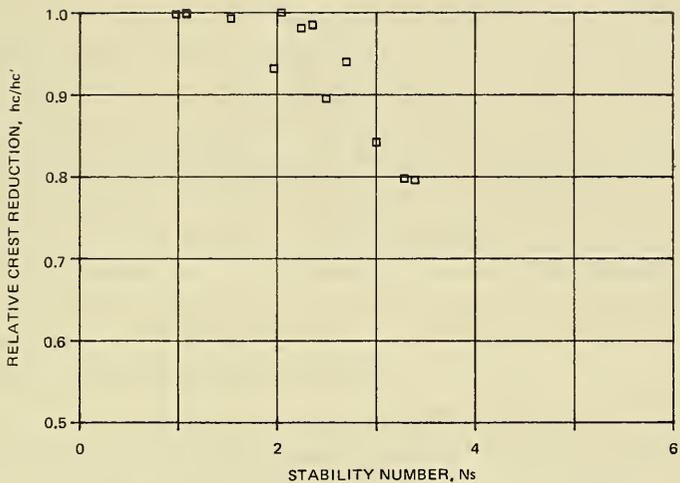
16

a. Crest height reduction factor versus the stability number
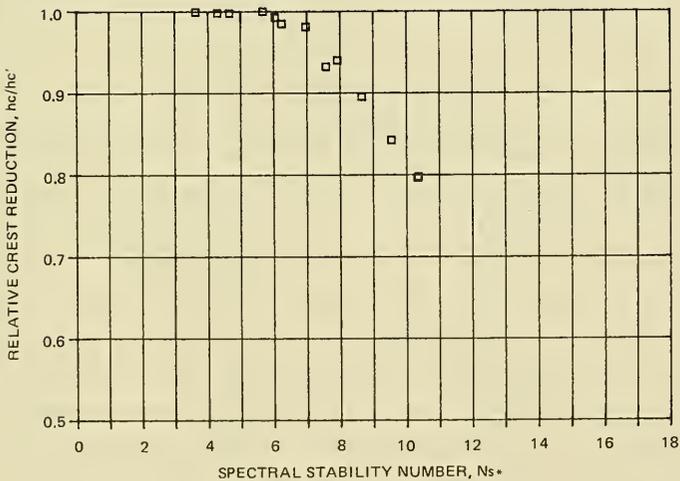
b. Crest height reduction factor versus the spectral stability number

Figure 8. Stability comparisons for subset 9

17

the relative severity of wave attack on reef breakwaters.

Secondary stability factors

21. Data analysis and observation of the laboratory tests indicate that several factors other than the spectral stability number have a quantifiable influence on the stability of reef breakwaters. Figure 9 will help identify what will be referred to as secondary stability factors or variables. In Figure 9 the damage trends for all five stability subsets are shown using subjectively drawn curves. Figure 9 shows the relative crest height h_c/d_s (see Figure 3) as a function of the spectral stability number. For intercomparing damage trends between subsets, the variable h_c/d_s is better than h_c/h_c' . When various subsets are plotted using h_c/h_c' , the data trends tend to fall on top of each other, especially for $N_s^* < 8$. Using h_c/d_s to show damage trends spreads the data out so that subsets can be distinguished and provides better orientation by showing the swl.

22. Relative exposure to wave action. One secondary stability factor is the relative exposure of the structure to wave action. Submerged breakwaters are much less exposed to wave attack than breakwaters with crests above the water level. Water overlying a submerged crest greatly dampens wave impact forces and attenuates the lift and drag forces on the stone. This factor is illustrated in Figure 9 where structures with the greater initial relative height h_c'/d_s have their height reduced more rapidly with increasing N_s^* than structures with lower initial relative height. In Table 4, which can be used with Figure 9 to evaluate the influence of secondary stability factors, the average value of initial relative crest height h_c'/d_s is given by subset along with two other secondary stability factors, the bulk number and the "as built" effective reef slope C' , which are discussed below. Subsets 1 and 5, which represent tests using the same stone size and water depth, illustrate the influence of h_c'/d_s on stability. Figure 9 shows that the wide difference in initial relative height of these structures is maintained until N_s^* is about 6.0; however, when noticeable stone movement starts at about N_s^* = 6 , the difference in relative heights for the reefs of the two subsets tends to decrease with increasing value of N_s^* . For the most severe conditions at about N_s^* = 17 , the difference in relative height between the two subsets is not very large. Based on analysis of all the data, it is concluded that the greater the initial height of the reef the more vulnerable it is to wave attack.
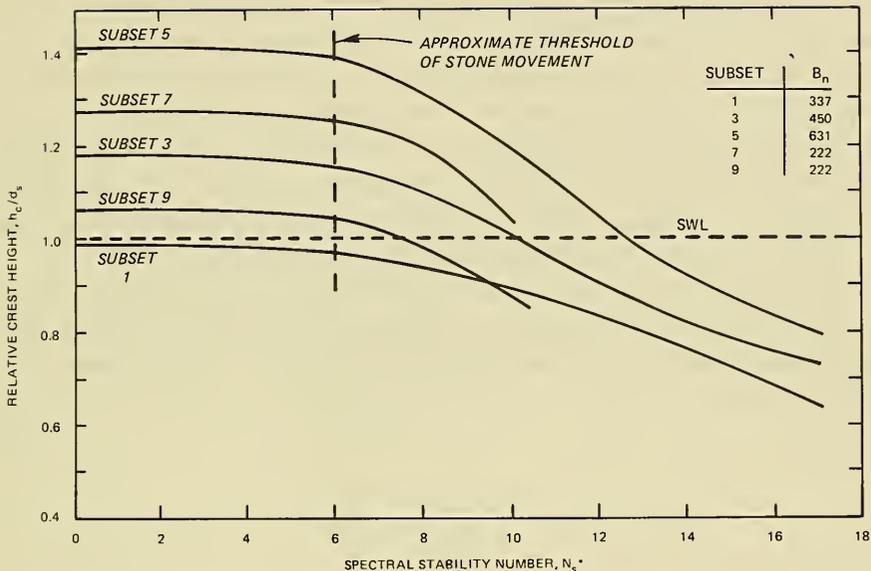
Figure 9. Damage trends of the relative crest height as a function of
the spectral stability number for the stability subsets 1, 3, 5, 7,
and 9

Table 4

Average Values of Secondary Stability Variables by Subset

Subset No.	Relative Crest Height "as Built" h'_c/d_s	Reef Size B_n *	Effective Reef Slope "as Built" C' **
1	0.99	337	1.90
3	1.18	450	1.80
5	1.41	631	1.76
7	1.27	222	1.88
9	1.06	222	1.88

* B_n bulk number, defined by Equation 3.

** C' effective reef slope, "as built," defined by Equation 4.

23. Influence of reef bulk. Subsets 1 and 5 can be used also to illustrate the influence of size or bulk of the reef on stability. Even though the difference in relative height for the two subsets narrows with increasing N_s^* , the crest heights of the reefs of subset 5 always are higher than those of subset 1. In fact, Figure 9 shows that the relative position of the trends for subsets 1, 3, and 5 are maintained such that the larger structure always has a greater crest height than the smaller structure for a given value of N_s^* . In order to intercompare the stability of all subsets, a general measure of breakwater size is needed which will be consistent with the data trends shown in Figure 9. Within this context, the variable which best characterizes the size of the reef breakwater is called the bulk number B_n and is defined as

$$ B_n = \frac{A_t}{\left(\dfrac{W_{50}}{w_r}\right)^{2/3}} = \frac{A_t}{d_{50}^2} \tag{3} $$

where

A_t = area of breakwater cross section, cm^2

w_r = unit weight of stone g/cm^3

d_{50} = dimension of stone, cm

24. Bulk number can be described as the equivalent number of median stones per median stone width in the breakwater cross section. Equivalent is used because B_n does not include the influence of porosity which is about 45 percent for the two stone gradations used in this study. The value of the bulk number lies in its ability to explain the rather straightforward behavior of the relative location of the damage trends for subsets 1, 3, and 5 in Figure 9. It also explains the rather anomalous behavior, such as that of the trend for subset 9 crossing the trend for subset 1. At first it seems surprising that the reefs of subset 9 degrade faster than those of subset 1, considering that the reefs of subset 9 have the greater cross-sectional area (see Table 2). However, when the bulk number is used to measure the size of the reef rather than the cross-sectional area, the relative behavior of the damage trends for subsets 1 and 9 seems more plausible. Subsets 1 and 9 have bulk numbers of 337 and 222, respectively, indicating that the reefs of subset 1

have more stone in the cross section than the reefs of subset 9. All the data appear to indicate that when the relative severity of wave attack is based on the spectral stability number the stability of the reef correlates better with the number of stones in the cross section than with the absolute size of the cross section. Other factors being equal, a reef with a large bulk number is more stable than a reef with a small bulk number because there are more stones to dissipate wave energy and to shelter other stones from wave forces.

25. <u>Effective slope of the reef.</u> The remaining secondary stability factor is a combination of the first two. This factor, referred to as the effective slope of the reef, is obtained by dividing the cross-sectional area by the square of the crest height. Two effective slope variables will be discussed in this report: (a) the effective slope of the structure "as built," defined as

$$C' = \frac{A_t}{h'^2_c} \tag{4}$$

and (b) the response slope for the reef breakwater to wave action, defined as

$$C = \frac{A_t}{h^2_c} \tag{5}$$

These variables are considered a cotangent function since dividing A_t by h_c one time produces a variable which can be regarded as a horizontal length, and dividing this length by h_c creates a cotangent-like variable. For low-crested, or submerged reefs, these variables provide a simple way to characterize an average slope or shape for what is sometimes a rather complex shape (e.g., see Figure 3). Table 4 shows that the average values of the effective structure slope "as built" are in a relatively narrow range. Since the landward and seaward faces of the reef were built to a slope of 1V on 1.5H (cot θ = 1.5), the difference between the values of C' in Table 4 and 1.5 result from the crest width of the trapezoid which increases the effective slope, as illustrated in Equation 6. The "as built" cross section of the reef is a narrow trapezoid with a crest width three stone diameters wide. For this study

21

the cross-sectional area of the reef is given approximately by

$$A_t = \left(h_c'\right)^2 \cot \theta + 3h_c' \left(\frac{W_{50}}{w_r}\right)^{1/3} \qquad (6)$$

where $\cot \theta$ is the cotangent of the angle θ between the "as built" seaward and landward breakwater slopes and the horizontal. If the severity of wave attack exceeds a value of the spectral stability number of about six, the reef deforms. A convenient method to quantify the deformation is to use effective response slope for reef breakwaters defined by Equation 5. In Figure 10 the response slope C is plotted as a function of N_s^*. This figure is similar to Figure 14.17 presented by Wiegel (1964) showing the relationships among the grain size, beach slope, and severity of the exposure of a beach to wave action.

26. Because of the narrow range of the effective "as built" reef slope C' (Table 4), it was not possible to quantify the influence of this variable on stability. It is assumed that the flatter the initial slope of the reef the more stable it will be. Future laboratory tests may expand the range of this variable so that the influence of the initial slope can be determined definitively.

27. Figure 10 suggests that a logical form for a reef breakwater stability equation would be

$$\frac{A_t}{h_c^2} = \exp \left(C_1 N_s^*\right) \qquad (7)$$

where C_1 is a dimensionless coefficient. Regression analysis was used to determine the value of C_1 for tests where $N_s^* > 6.0$; the value obtained was $C_1 = 0.0945$. With this value of C_1 , Equation 7 explains about 99 percent of the variance in C for the 109 stability tests with $N_s^* > 6.0$. Equation 7 approaches logical limits with

$$C \rightarrow \infty \ , \ \text{as} \ \ N_s^* \rightarrow \infty$$
and
$$C \rightarrow 1.0 \ , \ \text{as} \ \ N_s^* \rightarrow 0$$

22
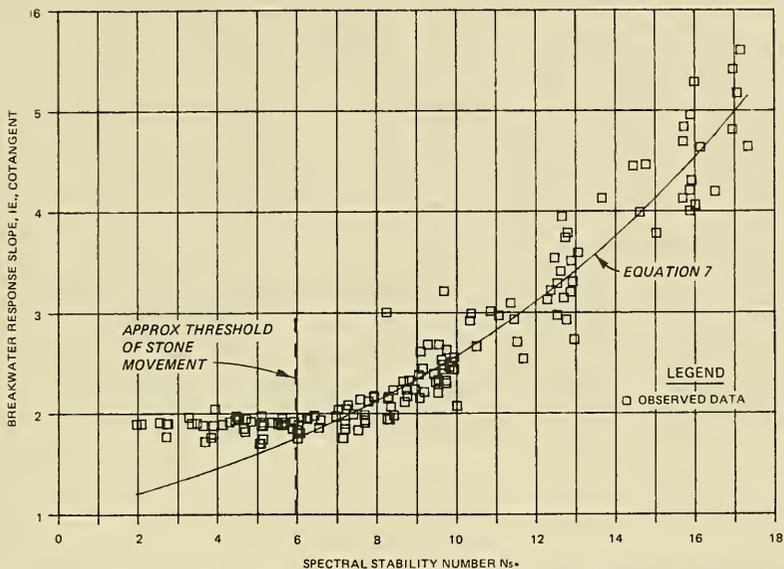
Figure 10. Reef breakwater response slope versus the spectral
stability number for stability subsets 1, 3, 5, 7, and 9

since the natural angle of repose for gravel is about 45 deg, giving C = 1.0
for a triangular reef cross section with side slopes of 1V on 1H.   Equation 7
can be compared to the observed data in Figure 10.   It is surprising that the
response slope of the reef, stone size and density, and severity of wave
attack can all be linked with a relation as simple as that in Equation 7.   It
is difficult to add secondary stability variables to an equation like Equa-
tion 7 and improve the ability to predict the response slope over Equation 7
very much.   At the same time it is clear from Figure 9 that secondary stabil-
ity factors have some influence on reef stability.   After trial and error the
following equation was developed which includes one secondary stability vari-
able and does a better job of predicting the response slope of the reef:

$$C = \frac{A_t}{h_c^2} = \exp \left\{ N_s^* \left[0.0676 + 0.0222 \left(\frac{h_c'}{d_s} \right) \right] \right\} \qquad (8)$$

where the relative "as built" crest height of the reef h_c'/d_s was added to an
equation like Equation 7 to improve the predictive ability.   Equation 8

23

explains 99.5 percent of the variance in C for the 109 tests with $N_s^* > 6$.

28. It was found that when using Equation 8 to predict the relative crest height h_c/d_s for values of N_s^* near or below six, illogically high values could result. Higher values are to be expected since Equation 6 was developed for tests where $N_s^* > 6$ and there was enough rock movement to form an equilibrium reef profile and not for wave conditions where the "as built" reef slope was too stable to be deformed. Since it would be useful to have a stability model which predicts reasonable response crest heights over the entire range of test conditions, another stability equation was developed to predict crest heights for values of $N_s^* < 10$. This range provides a con- venient overlap with the range of Equation 8 and allows an equation to be developed which will be simple enough to serve as a rule-of-thumb relation for zero to relatively low damage situations. This equation is given by

$$\frac{h_c}{h_c^t} = \exp\left[-0.00005 \ (N_s^*)^{3.5}\right] \tag{9}$$

Equation 9 provides a simple relation which follows the trend of the data well, albeit somewhat conservatively in the range $N_s^* < 10$ as can be seen in Figure 11. The small levels of damage predicted by Equation 9 for $N_s^* < 6$ represent settlement and consolidation of the reef under wave action and not conspicuous stone movement.

29. Equations 8 and 9 are used together to compute the response crest height of the reef over a wide range of wave severity. This approach will be referred to as the stability model. The procedure is to use Equation 8 for $N_s^* > 10$ and Equation 9 for $N_s^* < 6$. If we let the solution for h_c/h_c^t in Equation 9 be denoted $\left(h_c/h_c^t\right)_\ell$ and the solution for h_c/h_c^t in Equation 8 be denoted $\left(h_c/h_c^t\right)_u$, then the following equation

$$\left(\frac{10 - N_s^*}{10 - 6}\right)\left(\frac{h_c}{h_c^t}\right)_\ell + \left(\frac{N_s^* - 6}{10 - 6}\right)\left(\frac{h_c}{h_c^t}\right)_u \tag{10}$$

can be used in the transition region $6 < N_s^* < 10$ to compute the response crest height h_c. To judge the effectiveness of this procedure,

24
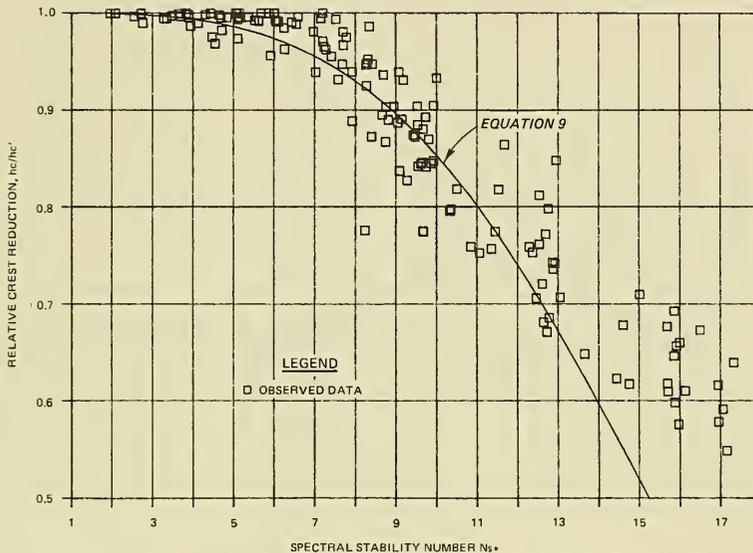
Figure 11. Crest height reduction factor versus spectral stability
number for stability subsets 1, 3, 5, 6, and 9

Figures 12, 13, 14, 15, and 16 were prepared to compare observed data for sub-
sets 1, 3, 5, 7, and 9, respectively, with synthetic data trends generated by
the stability model. Figures 12 through 16 show h_c/d_s versus N_s^* with
synthetic trends for each subset generated using A_t and d_s from Table 2
and h_c'/d_s from Table 4. Values of h_c/d_s were generated at integer values
of N_s^* for a range of N_s^* about the same as observed within each subset.
Synthetic damage trends comprise the type of information that could be gen-
erated by a user of the stability model. In general, synthetic trends follow
observed data trends very well. Discrepancies between predicted and observed
values appear to occur because the stability model does not include the bulk
number.
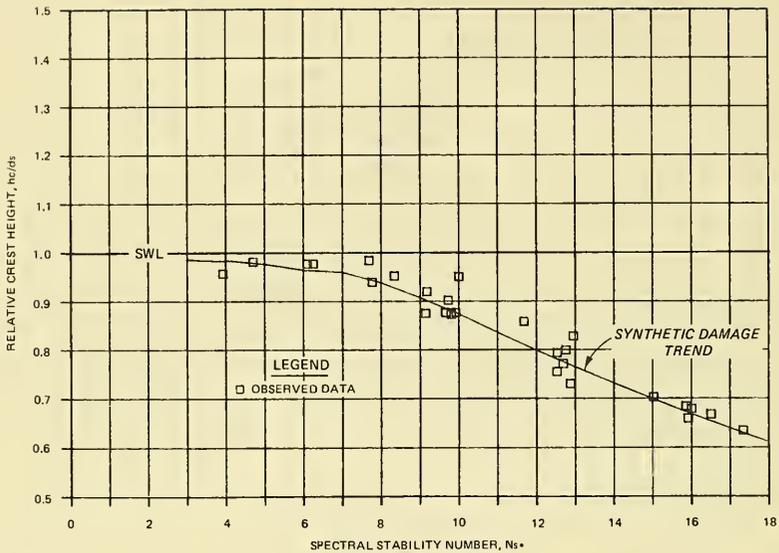
Figure 12. Comparison of data and the synthetic damage trends
generated by the stability model for subset 1
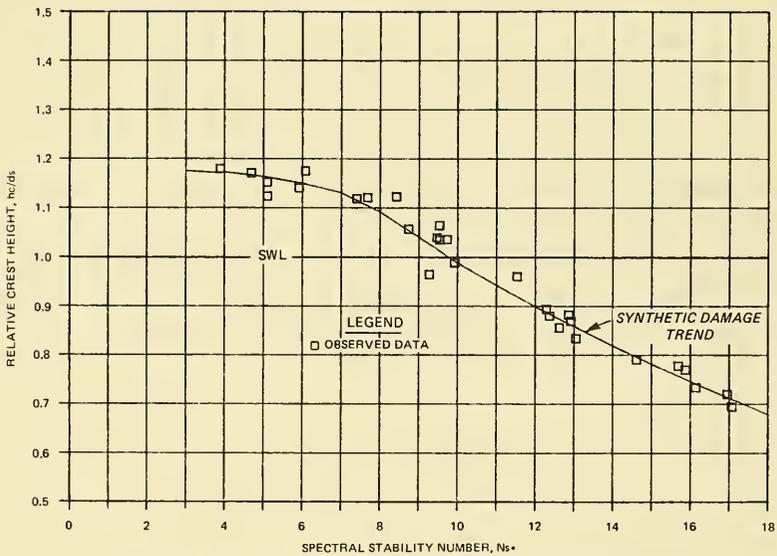
Figure 13. Comparison of data and the synthetic damage trends
generated by the stability model for subset 3

26
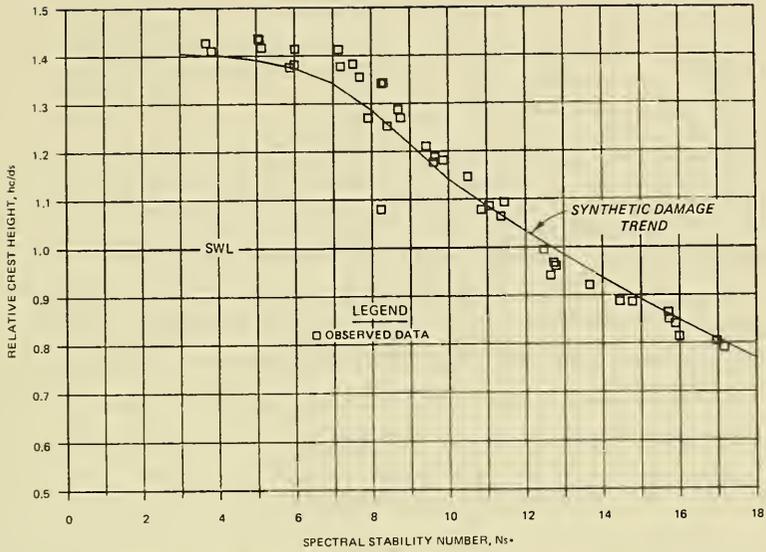
Figure 14. Comparison of data and the synthetic damage trends
generated by the stability model for subset 5
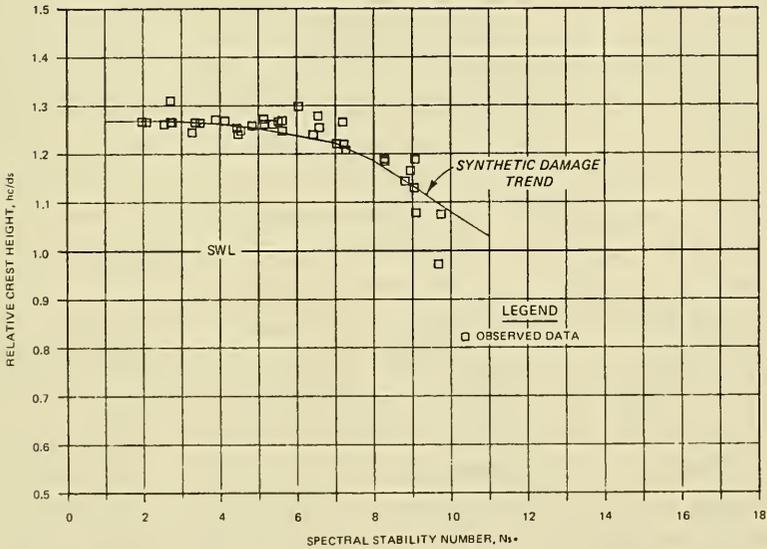
Figure 15. Comparison of data and the synthetic damage trends
generated by the stability model for subset 7

27
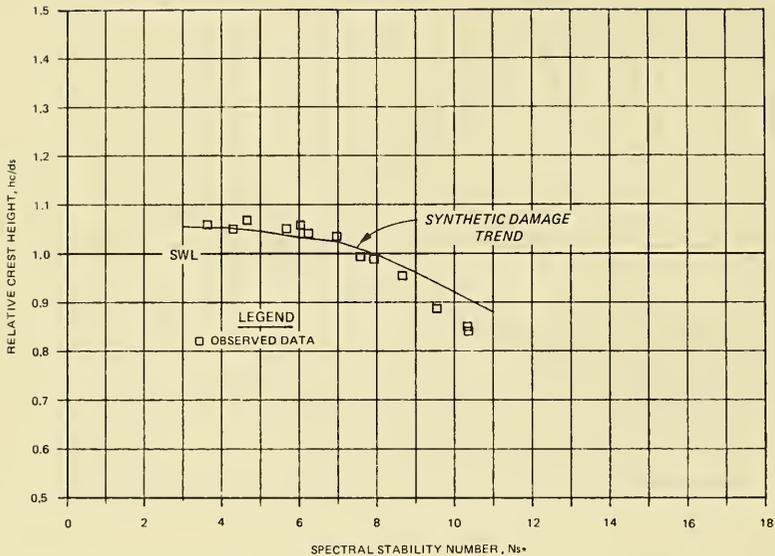
Figure 16. Comparison of data and the synthetic damage trends
generated by the stability model for subset 9

Wave Transmission

30. For the tests mentioned above the wave transmission coefficient K_t
is defined as

$$K_t = \frac{H_t}{H_c} \tag{11}$$

where H_t is the zero-moment transmitted wave height, and H_c is the zero-
moment wave height at the transmitted gage locations with no breakwater in the
test channel. Although this is not the most commonly used definition of K_t,
it has some advantages over the traditional definition which is given by the
ratio of transmitted to incident wave height. Equation 11 can be stated as
the ratio of the transmitted wave height to the wave height which would be
observed at the same location without the breakwater in the channel. This
definition eliminates wave energy losses occurring between the incident and
transmitted gages in the absence of a breakwater in the testing channel.

28

These losses were observed to be considerable for the most severe wave conditions during calibration of the channel. In effect, K_t measures attenuation of wave energy because of the presence of the breakwater and eliminates additional energy losses caused by natural wave breaking processes occurring between the incident and transmitted wave gages. Using the above definition of K_t will allow evaluation of wave energy dissipating characteristics of reef breakwaters in the next section. Because of the definition used, K_t should be somewhat conservative, i.e., higher than the more traditional definition of the transmission coefficient.

31. Wave transmission has proved to be a very difficult characteristic of reef breakwaters to predict partly because this study includes both submerged and nonsubmerged rubble-mound structures. Seelig (1980) found that the relative freeboard parameter F/H_{mo} was the most important variable in explaining wave transmission of submerged and overtopped breakwaters, where freeboard F is equal to crest height minus water depth, i.e., $F = H_c - d_s$. However, a confusing trend will be obtained using this variable when there is a transition in the dominant mode of transmission from that due to wave runup and overtopping to that due to transmission through the structure. Figure 17 identifies the dominant mode of transmission as a function of the relative freeboard and shows a schematized data trend. The difficulty in parameterizing the wave transmission process can be appreciated partly by considering the influence of the wave height. When a reef breakwater is submerged, the primary mode of transmission results from wave propagation over the crest and, generally, the smaller the wave the greater the K_t. When the crest is just above the water level, the dominant mode of transmission results from wave runup and overtopping, and the larger the wave the larger the K_t. If the relative freeboard is greater than about one, the dominant mode of transmission is through the structure; and the smaller the wave the greater the K_t. A number of other factors tend to further confuse the above generalities.

32. The easiest way to discuss development of a general wave transmission model for reef breakwaters is to first consider relatively high structures where relative freeboard F/H_{mo} is greater than one. When the dominant mode is wave transmission through the reef, K_t is a function largely of one variable which is the product of wave steepness and bulk number. Figure 18 shows a plot of K_t versus the reef transmission variable $\left(L_p \, d_{50}^2 \right) \Big/ (H_{mo} \, A_t)$ for the 37 tests where $F/H_{mo} > 1.0$. This one variable caused the wave

29
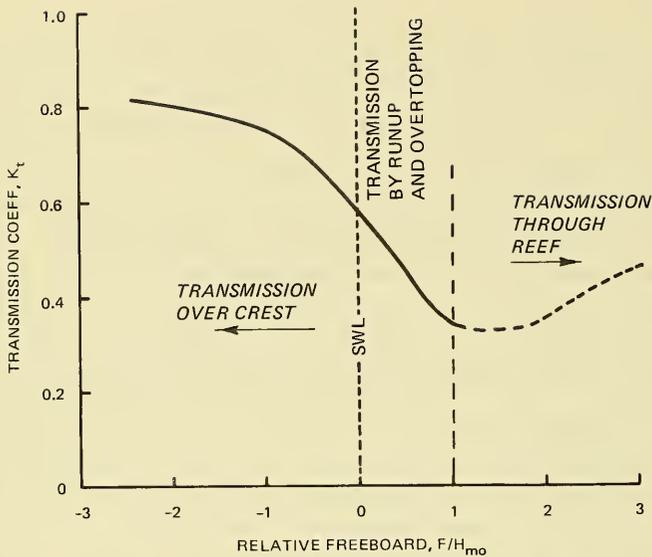
Figure 17. Conceptual sketch showing the dominant modes of wave transmission for a reef as a function of the relative freeboard
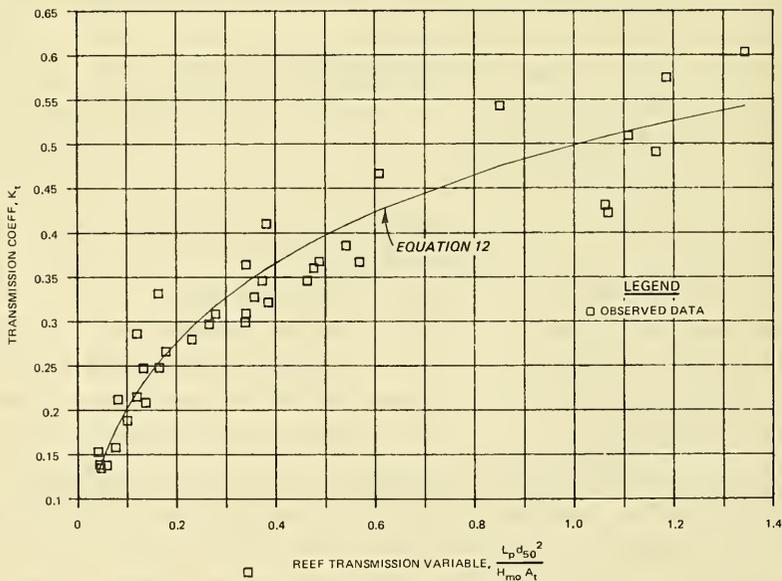
Figure 18. Wave transmission coefficient as a function of the reef transmission variable to illustrate the ability of Equation 12 to predict transmission of relatively high reefs ($F/H_{mo} > 1.0$)

30

transmission data to coalesce into one well-defined trend. A prediction equation was fit to the data shown in Figure 18, and the following relation was obtained:

$$K_t = \frac{1.0}{1.0 + \left(\dfrac{H_{mo} A_t}{L_p d_{50}^2}\right)^{0.592}} \qquad (12)$$

for

$$\frac{F}{H_{mo}} > 1.0$$

Equation 12 explains about 97 percent of the variance in K_t for the range considered. It is apparent from the composition of Equation 12 why the relative freeboard F/H_{mo} was not a good variable for explaining wave transmission through relatively high breakwaters.

33. For conditions where transmission is not dominated by wave energy propagating through the reef, relative freeboard F/H_{mo} is the most influential variable. Part of the value of the variable is in being able to account for the changing influence of wave height as the dominant mode of transmission shifts between wave propagation over the crest to wave runup and overtopping. For submerged reefs the relative freeboard correctly indicates the interesting property of being able to dissipate energy of large waves more effectively than that of small waves. For reefs being overtopped, the relative freeboard correctly indicates that larger waves have higher transmission coefficients. In spite of these assets, wave transmission for low and submerged reefs is far too complicated to be formulated adequately in terms of F/H_{mo} alone partly because wave energy is still propagating through low and submerged reefs even though transmission may be dominated by either overtopping or propagation over the crest. In addition, energy going over the reef is quite dependent on crest width and bulk of the structure which introduces the influence of other variables. Considering the multitude of confusing influences and the complexity of the phenomenon, the following regression relation was fit to the 167 tests with relative freeboards less than one:

31

$$K_t = \cfrac{1.0}{1.0 + \left(\cfrac{h_c}{d_s}\right)^{C_1} \left(\cfrac{A_t}{d_s L_p}\right)^{C_2} \quad \exp\left[C_3\left(\cfrac{F}{H_{mo}}\right) + C_4\left(\cfrac{A_t^{3/2}}{d_{50}^2 L_p}\right)\right]} \qquad (13)$$

for

$$\frac{F}{H_{mo}} < 1.0$$

where

$C_1 = 1.188$
$C_2 = 0.261$
$C_3 = 0.529$
$C_4 = 0.00551$

Equation 13 explains about 92 percent of the variance in K_t for the 167 tests where $F/H_{mo} < 1.0$. Equation 13 is the result of a considerable amount of trial and error effort to find an equation which fits the data well, makes physical sense based on current understanding of the phenomenon, approaches the correct limiting values, and is reasonably simple. The regression analysis for Equation 13 is shown in Appendix B.

34. If Equations 12 and 13 are used, the transmission coefficient can be predicted over the entire range of conditions tested in this study. Predicted values of K_t were made using Equation 12 for $F/H_{mo} > 1.0$ and Equation 13 for $F/H_{mo} < 1.0$. This prediction method will be referred to as the wave transmission model. Figures 19, 20, 21, 22, and 23 show predicted and observed values of K_t as a function of F/H_{mo} for subsets 1 and 2, 3 and 4, 5 and 6, 7 and 8, and 9 and 10, respectively. Figures 19 through 23 indicate that the wave transmission model does a good job of predicting individual test results and produces trends very similar to those of the observed data.

35. In addition to investigating the attenuation of wave energy passing over and through the reef, it is also possible to determine the relative shift in wave energy caused by the structure. The shift in wave energy is measured by the ratio of the period of peak energy density of the transmitted wave to the period of peak energy density of the incident wave. Figure 24 shows the shift in peak period as a function of relative freeboard. What is surprising
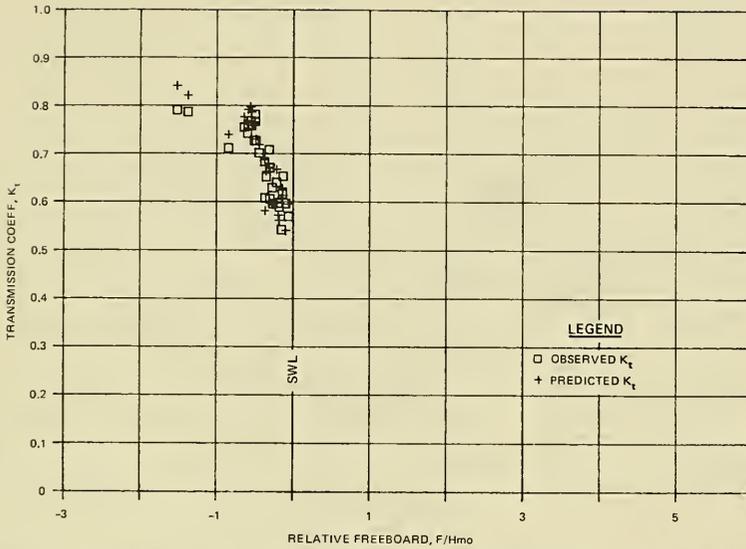
Figure 19. Comparison of data and predicted values of the wave transmission coefficient using the transmission model for subsets 1 and 2
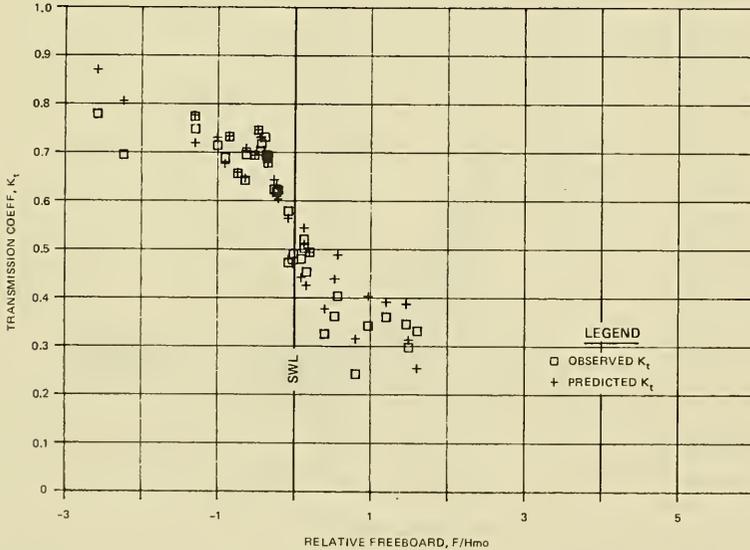
Figure 20. Comparison of data and predicted values of the wave transmission coefficient using the transmission model for subsets 3 and 4

33
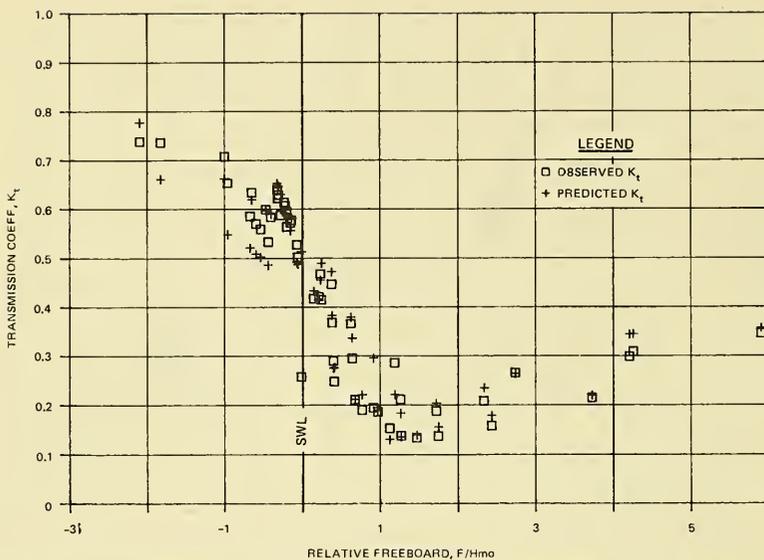
Figure 21. Comparison of data and predicted values of the wave transmission coefficient using the transmission model for subsets 5 and 6
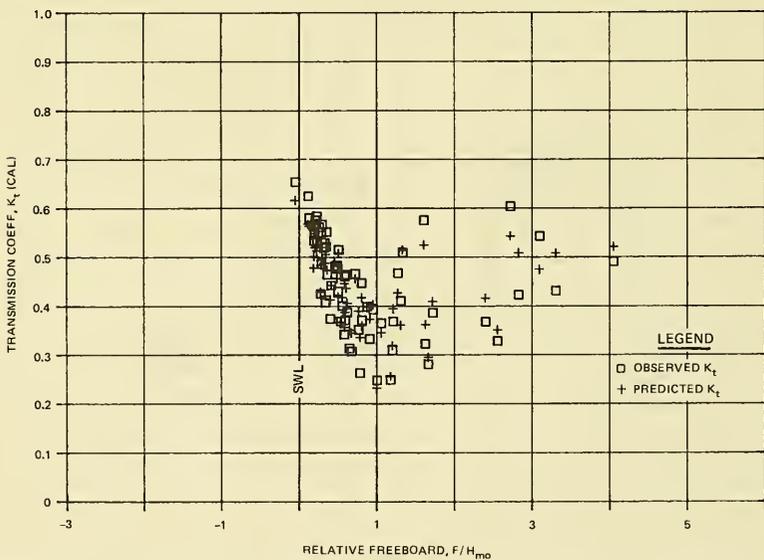
Figure 22. Comparison of data and predicted values of the wave transmission coefficient using the transmission model for subsets 7 and 8

34
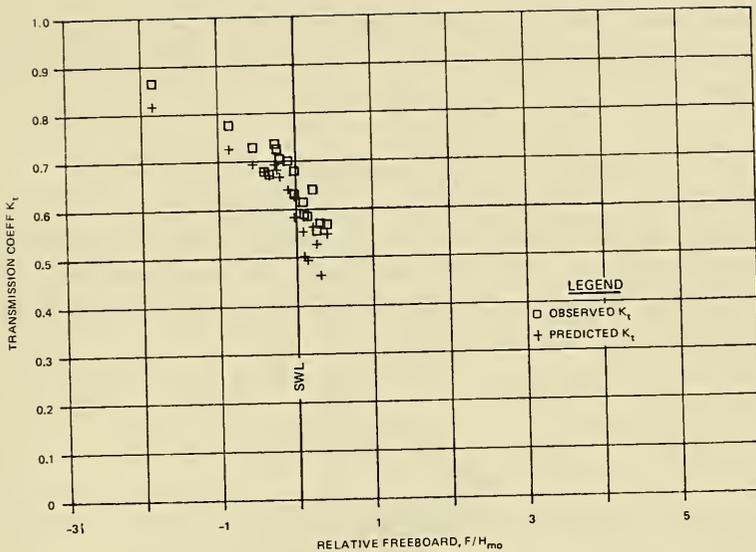
Figure 23. Comparison of data and predicted values of the wave trans-
mission coefficient using the transmission model for subsets 9 and 10
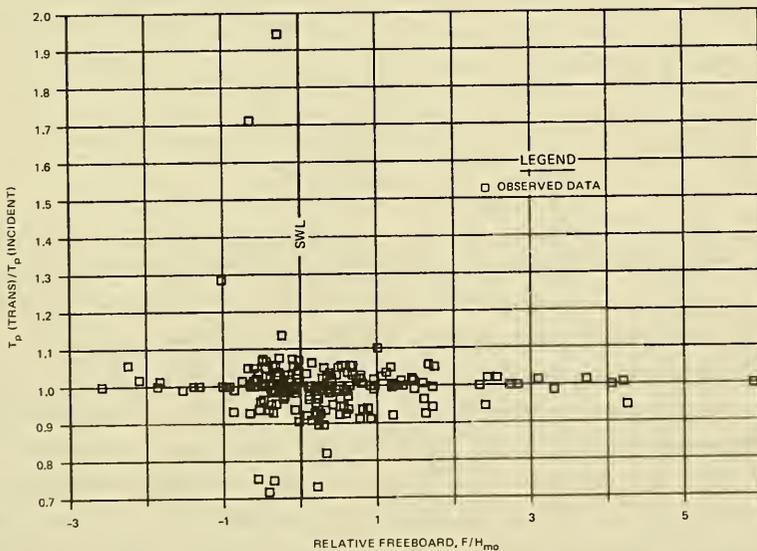
Figure 24. Ratio of the transmitted period of peak energy density to
the incident period of peak energy density as a function of the rela-
tive freeboard, all subsets

35

about this analysis is that the reef does not produce much shift in the peak
period of the spectrum. In fact, in only a few tests was the shift as much as
10 percent.

Wave Reflection and Energy Dissipation

36. The method developed by Goda and Suzuki (1976) to resolve the wave
spectrum into incident and reflected components is the method used in this
study to calculate the reflection coefficient. According to Goda and Suzuki,
the reflection coefficient is defined as

$$K_r = \sqrt{\frac{E_r}{E_I}}$$

where E_r and E_I are the reflected and incident wave energy of the spec-
trum, respectively.

37. One variable, the reef reflection parameter, was found to be con-
spicuously better than others for predicting wave reflection and is formulated
as

$$\frac{h_c^2 L_p}{A_t d_s} = \frac{L_p}{\left(\dfrac{A_t}{h_c^2}\right) d_s}$$

This parameter can be thought of as approximately the ratio of wave length to
horizontal distance between the toe of the reef and the swl on the reef.
Since, for many tests, the reefs are deformed and/or submerged, the quantity
$\left(A_t/h_c^2\right)d_s$ is sometimes only indicative of this horizontal distance. When K_r
is plotted versus the reef reflection parameter, a very strong data trend re-
sults (Figure 25). Such a strong trend seems surprising considering the com-
plex nature of irregular wave reflection and the wide range of conditions
represented in Figure 25. A regression equation was fit to the data shown in
Figure 25 to provide a convenient rule-of-thumb method to estimate reflection
from a reef and to provide insight relating to wave reflection from coastal
structures in general. The equation is given by

$$K_r = \cfrac{1.0}{1.0 + C_1\left(\cfrac{h_c^2 L_p}{A_t d_s}\right)^{C_2}} \qquad (14)$$

where $C_1 = 8.284$ and $C_2 = -0.951$ are coefficients. Equation 14 explains about 80 percent of the variance in K_r for the 204 tests considered, follows the trend of the data well, and approaches the correct limiting values.
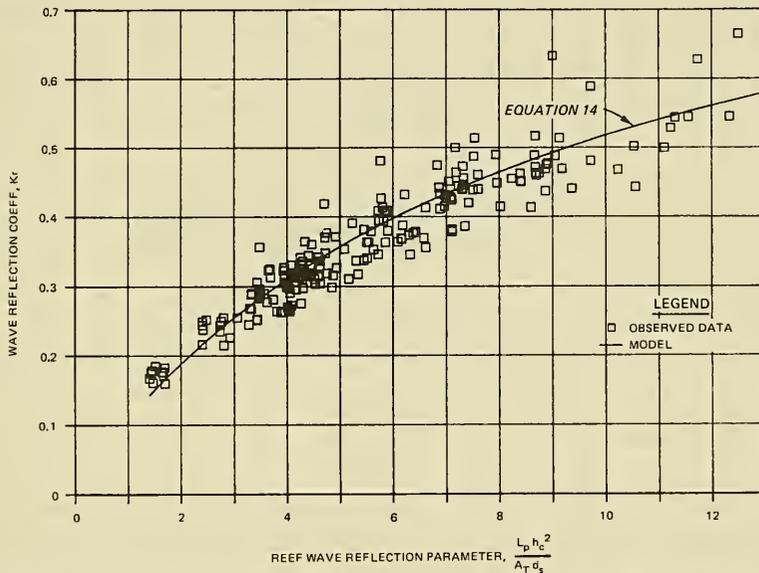
Figure 25. Wave reflection coefficient versus the reef reflection parameter illustrating the ability of Equation 14 to predict reflection, all subsets

38. While the analysis was being conducted to develop Equation 14, it was clear a relation could be developed which could explain considerably more of the variance in K_r if more dependent variables were used. Better esti-mates of reflection from reefs would be valuable since wave reflection causes navigation problems, increases potential for toe scour, and can cause erosion at nearby shorelines by increasing the severity of wave conditions. In addi-tion, knowledge of wave reflection provides a way to estimate the amount of wave energy dissipated by the reef. The ability of low and submerged rubble structures to dissipate wave energy has long been appreciated, but only in

37

recent years has it been possible to quantify this property. Quantification of energy dissipation by a reef is the property that justified consideration of rubble-mound construction since both wave reflection and transmission are usually undesirable. The basic conservation of energy relation for rubble structures can be written as follows:

$$K_t^2 + K_r^2 + \text{dissipation} = 1.0 \tag{15}$$

where dissipation in Equation 15 refers to the fraction of the incident wave energy dissipated by the structure.

39. The following regression equation will provide an accurate estimate of wave reflection from a reef breakwater:

$$K_r = \exp\left[C_1\left(\frac{d_s}{L_p}\right) + \frac{C_2}{\frac{h_c}{d_s}} + C_3\left(\frac{A_t}{h_c^2}\right) + C_4\left(\frac{F}{H_{mo}}\right)\right] \tag{16}$$

where

$$C_1 = -6.774$$
$$C_2 = -0.293$$
$$C_3 = -0.0860$$
$$C_4 = +0.0833$$

Equation 16 explains about 99 percent of the variance in K_r for the 204 tests considered. The dependent variables and the signs of their coefficients are consistent with current understanding of wave reflection. All the dependent variables in Equation 16 affect reflection in a monotonic manner such that, other factors being equal, K_r increases as d_s/L_p decreases, h_c/d_s increases, A_t/h_c^2 decreases, and F/H_{mo} increases. However, some care should be exercised in using Equation 16; for example, reflection will increase with increasing crest height only until the crest height approaches the limit of wave runup which for a reef would be $F/H_{mo} \gtrsim 1.5$. Since all terms in Equation 16 are negative for submerged reefs, the equation approaches the correct limiting value of $K_r = 0$ for decreasing structure height. On the other hand, Equation 16 was fit to a data set where reflection was strongly correlated to height of the reef which suggests that the equation might not be satisfactory for reefs with crest heights above the limit of runup. This

problem is demonstrated in Figure 26a where the difference between predicted K_r and observed K_r are plotted versus relative freeboard F/H_{mo}. Figure 26a shows that Equation 16 predicts K_r usually to within ±0.05 with little systematic error except for high relative freeboards, i.e., $F/H_{mo} > 2.5$. Because of the possibility of systematic error for high relative freeboards, it is recommended that if the relative freeboard exceeds 2.5, a value of 2.5 be used in Equation 16. When this procedure is applied to the data of this study, it removes the systematic error as shown in Figure 26b.

40. It is intended that the prediction equation for K_r, Equation 16, be used with the wave transmission model (discussed in paragraph 34) in the energy conservation relation given by Equation 15 to compute energy dissipated by the reef. This approach was used to prepare Figure 27 which shows a scatter plot of predicted energy dissipation versus "observed" energy dissipation caused by the reef. Figure 27 shows that the procedure outlined above can make good predictions of energy dissipation and the rather surprising fact that, for some conditions, the reef can dissipate up to 90 percent of incident wave energy. Generally, greatest energy dissipation was observed for short-period waves on reefs which were high enough not to be overtopped. The lowest observed energy dissipation of about 30 percent occurred for the few reefs with a relative crest height less than 0.7, i.e., $h_c/d_s < 0.7$. For submerged reefs, energy dissipation increases with increasing steepness H_{mo}/L_p and with increasing relative reef width $A_t/d_s L_p$. Reefs with their crest near the swl will dissipate between about 35 to 70 percent of incident wave energy, and dissipation is strongly dependent on relative reef width as shown in Figure 28. For reefs with moderate to heavy overtopping, i.e., $0 < F/H_{mo} < 1.0$, energy dissipation is strongly dependent on the relative reef width but not on wave steepness.

41. Since wave energy dissipation characteristics of reef breakwaters are so important, a special analysis was conducted to illustrate the influence of the most important variables in a simple way that would still be consistent with the data. This analysis used the most effective two variables in predicting K_t and the two most effective variables for predicting K_r with the provision that one of the variables be common to both K_t and K_r so that the predicted values could be plotted on a common axis. Fortunately, the relative crest height h_c/d_s provides a good common variable. Good predictions are obtained for transmission using the variables h_c/d_s and B_n and for

39
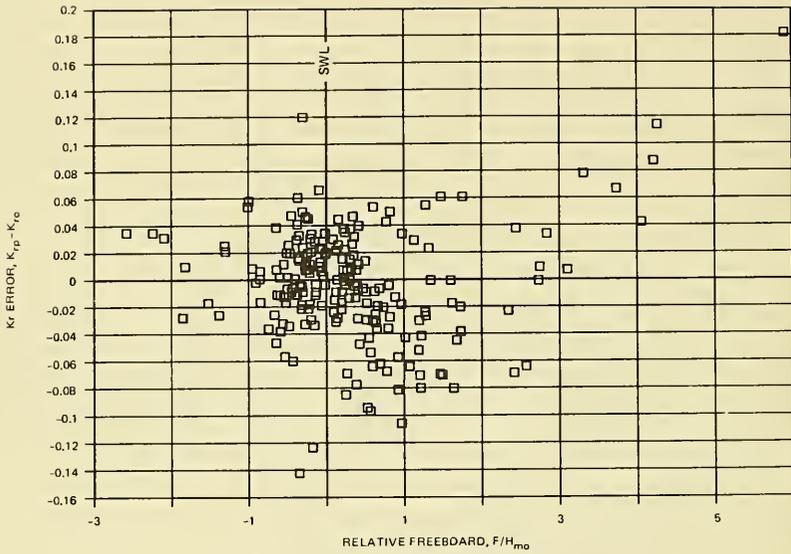
a. No upper bound for F/H_{mo}
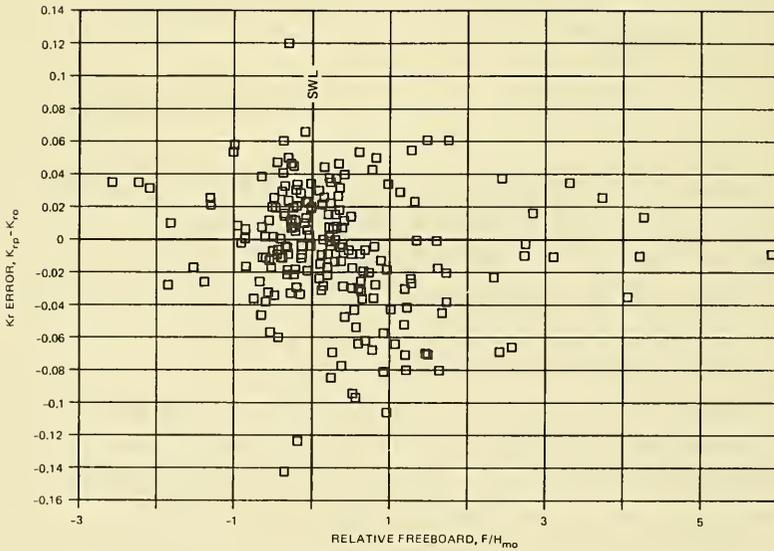
b. As upper bound, $F/H_{mo} = 2.5$

Figure 26. Error in predicting the reflection
coefficient using Equation 16

40
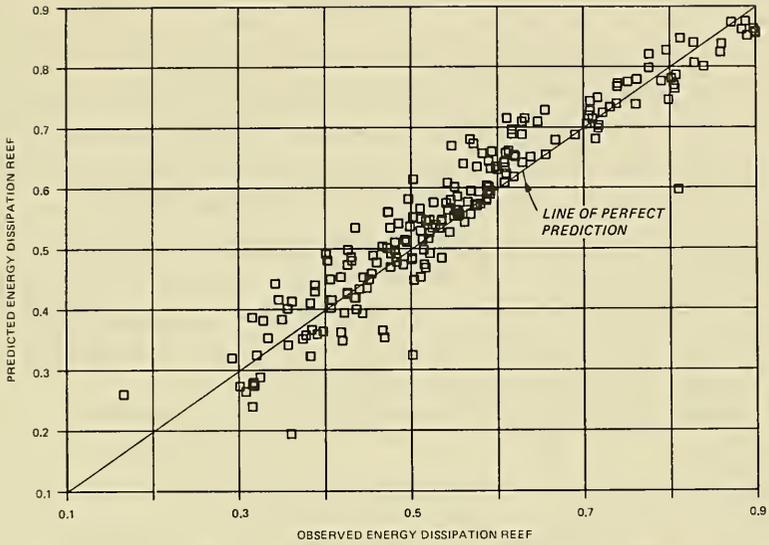
Figure 27. Scatter plot of the predicted energy dissipation by a reef using the dissipation model versus the observed energy dissipation, all subsets
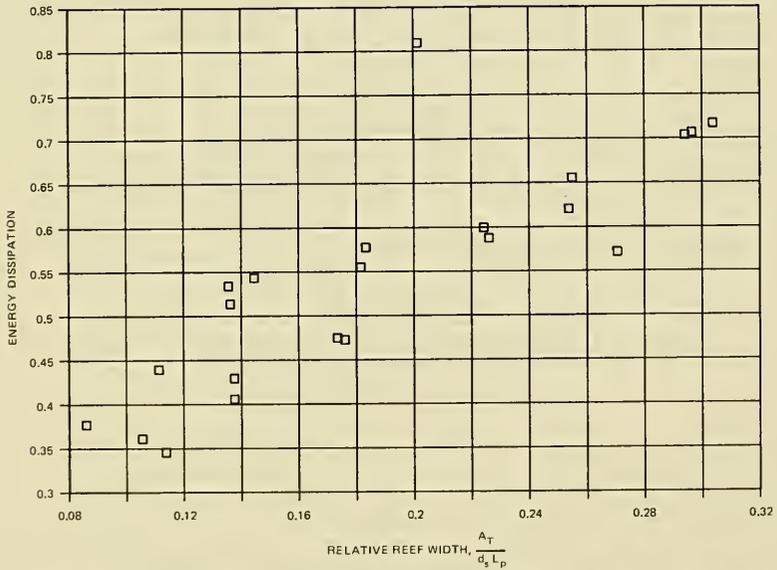
Figure 28. Energy dissipation by reefs with crest near the swl as a function of the relative reef width

wave reflection when h_c/d_s and relative depth d_s/L_p are used. Regression analysis was used to develop the curves for K_t and K_r shown in Figure 29. The equations used to compute the curves in Figure 26 explain about 82 percent and 98 percent of the variance in K_t and K_r , respectively. Appendix B gives the equations used in Figure 29 and other information related to the regression analysis. The curves shown in Figure 29 fit the general trends of the data quite well. However, the real value of Figure 29 is that it is a compilation of information about wave transmission, wave reflection, and wave energy dissipation of reef breakwaters. Figure 29 is an improvement over Figure 8 in Ahrens (1984) because Figure 29 is based on an analytic model; whereas Figure 8 is based on subjective curve fitting to the observed data.
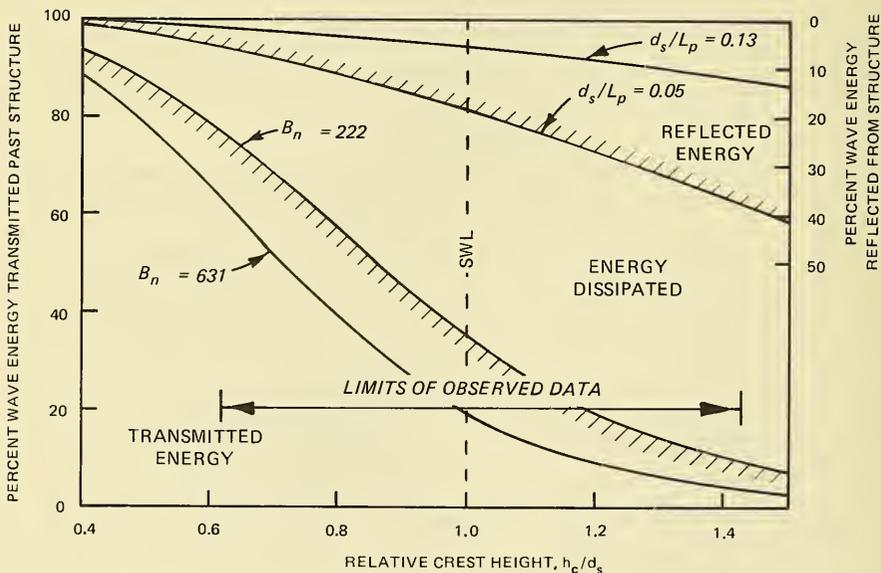
Figure 29.   Distribution of wave energy in the vicinity
of a reef breakwater

42

PART IV: CONCLUSIONS

42. This report summarizes the results from 205 laboratory tests of reef breakwaters conducted using irregular waves. Findings from this study can be categorized as follows: (a) the stability of the structure to wave attack, (b) wave transmission over and through the structure, (c) wave reflection from the structure, and (d) energy dissipation by the structure. These findings are largely summarized through the use of equations fit to the data which can be used to predict various breakwater characteristics with surprisingly high accuracy.

43. The important conclusions from this study are:

   a. A stability number was defined by Equation 2 and named the spectral stability number which was found to be the single most important variable influencing the stability of reef breakwaters.

   b. There is very little stone movement or damage for spectral stability numbers less than six, but stone movement and damage can be clearly seen for values greater than eight.

   c. For values of the spectral stability number above six, the influence of other variables on stability can be identified. Other factors being equal, the stability of the reef increases the lower the relative crest height h_c/d_s ; as its size defined by Equation 3 increases; and as the slope of the structure, as defined either by Equation 4 or 5, gets flatter.

   d. Wave transmission over and through a reef is a very complex process. Part of the complexity relates to the confusing influence of some variables; e.g., for breakwaters with positive freeboards transmission over the reef is directly proportional to wave height, while energy transmitting through the reef is inversely proportional to the wave height. For conditions where transmission is dominated by wave energy propagating through the reef, a simple relation, Equation 12, was found to predict the transmission coefficient very well. When the dominant modes of transmission resulted from wave overtopping or wave propagation over the crest of a submerged reef, a rather complex relation, Equation 13, was required to make reasonable estimates of transmission coefficients.

   e. Wave reflection is easier to predict than either stability or wave transmission. A simple relation using only one variable, Equation 14, was able to explain about 80 percent of the variance in the reflection coefficients. A more complex relation, Equation 16, was developed which explained about 99 percent of the variance in the reflection coefficient. Other factors being equal, reflection coefficients increase with increasing wave length and increasingly steeper reef slopes. Reflection

43

coefficients also increase with increasing relative reef height h_c/d_s and increasing relative freeboard F/H_{mo} until the crest height reaches the upper limit of wave runup.

f. Wave energy dissipation characteristics of a reef are difficult to summarize briefly because of the complexity of the phenomenon. One surprising finding was that for short-period waves $d_s/L_p > 0.12$ which do not overtop the crest the reef will dissipate 80 to 90 percent of incident wave energy. For reefs with the lowest relative crest height tested $0.63 < h_c/d_s < 0.70$, the structure would dissipate about 30 percent of incident wave energy. Reefs with their crests near the still-water level will dissipate between 30 to 70 percent of incident wave energy depending on the relative reef width $A_t/d_s L_p$.

The model developed in this study was found to make good estimates of energy dissipation.

REFERENCES

Ahrens, J. P. 1984 (Sep). "Reef Type Breakwaters," Proceedings of the 19th Coastal Engineering Conference, Houston, Tex., pp 2648-2662.

Allsop, N. W. H. 1983 (Mar). "Low-Crest Breakwater, Studies in Random Waves," Proceedings of Coastal Structures 83, Arlington, Va., pp 94-107.

Bremner, W. D., Foster, N., Miller, C. W., and Wallace, B. C. 1980. "The Design Concept of Dual Breakwaters and its Application to Townsville, Australia," Proceedings of the 17th Coastal Engineering Conference, Sydney, Australia, Vol 2, pp 1898-1908.

Goda, T., and Suzuki, Y. 1976. "Estimation of Incident and Reflected Waves in Random Wave Experiments," Proceedings of the 15th Coastal Engineering Conference, Honolulu, Hawaii, pp 828-845.

Gravesen, H., Jensen, O. J., and Sorensen, T. 1980. "Stability of Rubble Mound Breakwaters II," Danish Hydraulic Institute, Copenhagen, Denmark.

Hudson, R. Y., and Davidson, D. D. 1975. "Reliability of Rubble-Mound Breakwater Stability Models," Proceedings of the ASCE Symposium on Modeling Techniques, San Francisco, Calif., pp 1603-1622.

Lillevang, O. J. 1977 (Mar). "A Breakwater Subject to Heavy Overtopping: Concept, Design, Construction, and Experience," Proceedings of ASCE Specialty Conference, Ports '77, Long Beach, Calif., pp 1-33.

Lording, P. T. and Scott, J. R. 1971 (May). "Armor Stability of Overtopped Breakwater," Journal of Waterways, Harbors and Coastal Engineering, American Society of Civil Engineers, Vol WW2, Paper 8138, pp 341-354.

Raichlen, F. 1972 (May). "Armor Stability of Overtopped Breakwater," Journal of Waterways, Harbors, and Coastal Engineering, American Society of Civil Engineers, Vol WW2, Discussion of paper 8138, pp 273-279.

Seelig, W. N. 1979 (Mar). "Effect of Breakwaters on Waves: Laboratory Tests of Wave Transmission by Overtopping," Proceedings of Coastal Structures '79, Alexandria, Va., Vol 2, pp 941-961.

Seelig, W. N. 1980 (Jun). "Two-Dimensional Tests of Wave Transmission and Reflection Characteristics of Laboratory Breakwaters," CERC Technical Report No. 80-1, US Army Engineer Waterways Experiment Station, Vicksburg, Miss.

Vincent, C. L. 1981 (Nov). "A Method for Estimating Depth-Limited Wave Energy, Coastal Engineering Technical Aid 81-6, US Army Engineer Waterways Experiment Station, Vicksburg, Miss.

Walker, J. R., Palmer, R. Q., and Dunham, J. W. 1975 (Jun). "Breakwater Back Slope Stability," Proceedings of Civil Engineering in the Oceans/III, Newark, Del., Vol 2, pp 879-898.

Wiegel, R. L. 1964. Oceanographical Engineering, Prentice-Hall, Inc., Englewood Cliffs, N. J.

Wiegel, R. L. 1982 (Mar). "Breakwater Damage by Severe Storm Waves and Tsunami Waves," Prepared for Pacific Gas and Electric Co., Berkeley, Calif.

QUARTZITE   DIORITE
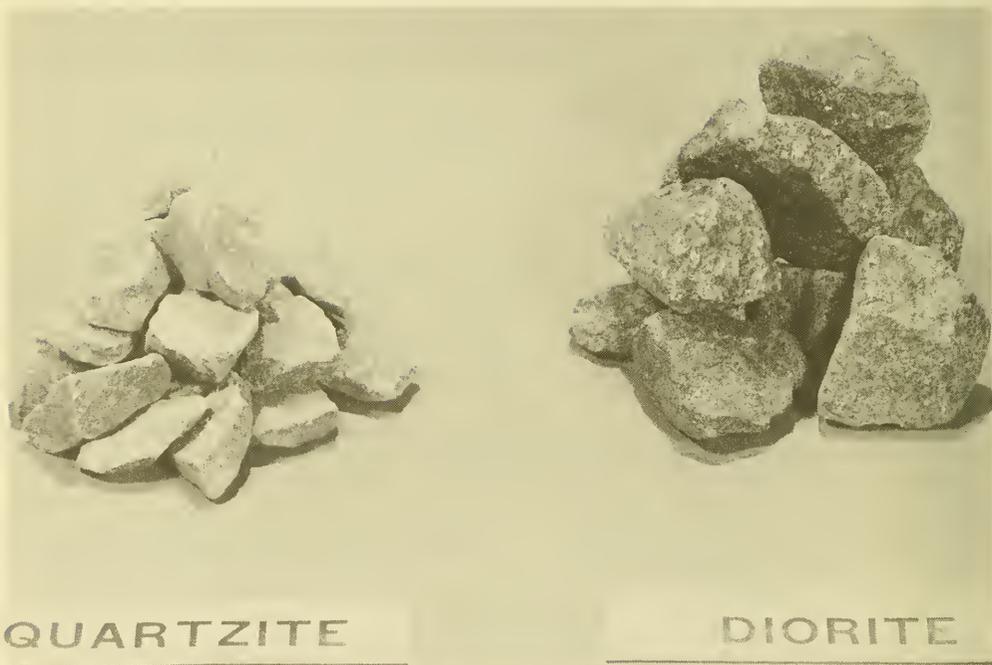
Photo 1. Representative samples of the stone used in this study
(As a scale, labels in figure are 12.2 by 2.3 cm.)

APPENDIX A: TABULAR SUMMARY OF STABILITY AND PERFORMANCE DATA

Subset NO.	Test NO.	Test Type	File And Gain	Median Weight W50 Stone gr.	Density Of Stone wt.	Area Of BW,At cm^2	Water Depth ds cm.	AVE. INC. Hmo cm.	AVE. INC. Tp sec.	AVE. Trans. Hmo cm.	AVE. Kr	Cal. Hmo cm.	Structure as Built hc cm.	Damaged Height Structure hc cm.	Area Of Damage Ad cm^2
1	1	1	1.100	17	2.630	1170	25	11.010	1.450	6.450	0.242	10.250	24.900	21.920	49.520
1	2	1	1.080	17	2.630	1170	25	10.140	1.460	5.680	0.231	9.500	24.720	23.010	42.920
1	3	1	1.060	17	2.630	1170	25	8.000	1.430	4.460	0.387	7.560	24.110	23.500	17.740
1	4	1	1.040	17	2.630	1170	25	5.730	1.450	3.270	0.210	5.480	25.390	24.440	10.590
1	5	1	1.020	17	2.630	1170	25	2.870	1.440	1.680	0.204	2.760	24.260	23.930	4.830
1	6	1	2.100	17	2.630	1170	25	13.430	2.230	8.230	0.332	11.620	24.410	20.700	77.200
1	7	1	2.080	17	2.630	1170	25	11.500	2.230	7.210	0.217	10.750	24.840	21.460	75.990
1	8	1	2.060	17	2.630	1170	25	9.070	2.250	5.800	0.379	8.880	25.480	23.770	34.750
1	9	1	2.040	17	2.630	1170	25	6.090	2.270	3.460	0.401	6.070	25.090	24.600	13.390
1	10	1	2.020	17	2.630	1170	25	2.910	2.280	1.580	0.413	2.910	24.990	24.540	8.640
1	11	1	2.100	17	2.630	1170	25	13.130	2.230	7.890	0.327	11.540	25.050	19.990	91.790
1	13	1	3.100	17	2.630	1170	25	15.780	3.000	9.360	0.311	11.970	25.730	16.980	213.030
1	14	1	3.080	17	2.630	1170	25	14.350	3.000	8.500	0.296	11.680	24.780	17.590	168.530
1	15	1	3.060	17	2.630	1170	25	11.380	2.780	7.200	0.299	10.260	24.440	19.840	100.610
1	16	1	3.040	17	2.630	1170	25	7.810	2.760	5.040	0.337	7.510	25.270	22.560	39.580
1	17	1	3.020	17	2.630	1170	25	3.890	2.750	2.360	0.425	3.830	24.660	24.440	2.040
1	18	1	3.100	17	2.630	1170	25	15.720	2.950	9.170	0.303	11.960	24.690	17.100	70.010
1	20	1	4.020	17	2.630	1170	25	5.460	3.530	3.400	0.461	5.310	24.140	23.800	5.950
1	21	1	4.040	17	2.630	1170	25	10.070	3.520	6.840	0.354	9.220	24.780	18.870	111.860
1	22	1	4.060	17	2.630	1170	25	14.250	3.600	8.890	0.322	11.690	25.120	16.490	181.720
1	23	1	4.070	17	2.630	1170	25	16.100	3.640	9.470	0.331	12.330	24.840	15.880	212.380
1	25	1	1.100	17	2.630	1170	25	11.450	1.450	6.330	0.240	10.620	24.220	21.920	35.770
1	26	1	1.080	17	2.630	1170	25	10.080	1.460	5.730	0.229	9.450	24.570	21.880	40.040
1	27	1	2.060	17	2.630	1170	25	8.870	2.240	5.650	0.483	8.670	25.090	21.820	43.290
1	28	1	3.060	17	2.630	1170	25	11.550	2.800	7.540	0.312	10.370	24.990	19.290	102.660
1	29	1	4.040	17	2.630	1170	25	10.380	3.590	7.130	0.338	9.440	24.810	18.260	131.180
1	30	1	4.060	17	2.630	1170	25	14.980	3.630	9.080	0.330	11.980	24.810	16.700	204.110
3	31	1	1.100	17	2.630	1560	25	11.360	1.470	5.180	0.234	10.540	29.170	24.720	119.380
3	32	1	1.080	17	2.630	1560	25	9.460	1.450	4.040	0.237	8.900	30.480	26.430	105.720
3	33	1	1.060	17	2.630	1560	25	7.820	1.440	2.420	0.299	7.430	29.600	28.040	44.870
3	34	1	1.040	17	2.630	1560	25	5.500	1.440	1.280	0.319	5.270	29.630	29.380	5.650
3	35	1	1.020	17	2.630	1560	25	2.820	1.440	0.720	0.338	2.170	29.630	29.500	7.340
3	36	1	3.100	17	2.630	1560	25	15.630	2.980	8.220	0.303	11.950	29.810	19.260	299.890
3	37	1	3.080	17	2.630	1560	25	13.760	3.000	7.980	0.288	11.480	29.170	19.780	303.420
3	38	1	3.060	17	2.630	1560	25	10.980	2.810	6.180	0.319	10.000	29.440	22.340	155.890
3	39	1	3.040	17	2.630	1560	25	7.490	2.820	3.760	0.430	7.220	29.260	25.880	67.730
3	40	1	3.020	17	2.630	1560	25	3.680	2.790	1.240	0.584	3.620	29.840	28.530	23.230
3	41	1	2.100	17	2.630	1560	25	13.380	2.230	7.180	0.311	11.610	29.290	21.730	175.400
3	42	1	2.080	17	2.630	1560	25	11.170	2.270	6.100	0.331	10.540	29.380	24.020	122.260
3	43	1	2.060	17	2.630	1560	25	8.350	2.250	4.140	0.411	8.230	29.810	26.000	77.760
3	44	1	2.040	17	2.630	1560	25	5.720	2.290	2.070	0.510	5.710	29.290	27.980	34.000
3	45	1	2.020	17	2.630	1560	25	2.890	2.280	0.860	0.532	2.890	29.440	29.290	2.890
3	46	1	4.020	17	2.630	1560	25	5.510	3.560	2.160	0.597	5.350	29.630	28.070	29.640
3	47	1	4.040	17	2.630	1560	25	10.610	3.580	7.030	0.339	9.610	29.500	20.850	244.610
3	48	1	4.040	17	2.630	1560	25	10.170	3.520	6.300	0.344	9.290	29.690	21.400	208.010
3	49	1	4.060	17	2.630	1560	25	14.610	3.570	8.330	0.328	11.840	30.080	18.350	341.420
3	50	1	4.070	17	2.630	1560	25	15.820	3.600	9.140	0.332	12.250	29.380	17.370	345.880
3	51	1	4.010	17	2.630	1560	25	2.610	3.520	0.890	0.615	2.570	28.990	28.800	5.390
3	52	1	2.100	17	2.630	1560	25	13.230	2.250	7.200	0.320	11.570	29.690	22.070	177.540
3	54	1	3.100	17	2.630	1560	25	15.590	2.900	8.290	0.305	11.950	28.740	19.450	258.270
3	56	1	4.070	17	2.630	1560	25	15.840	3.520	8.800	0.317	12.260	29.230	18.010	332.960

Note: Area of BW = cross-sectional area of breakwater; Inc. H_{mo} = incident H_{mo}; Inc. T_p = incident T_p; Trans. H_{mo} = transmitted H_{mo}; Cal. H_{mo} = calibrated H_{mo}.

Subset NO.	Test NO.	Test Type	File And Gain	Median Weight W50 gr.	Density Of Stone wt.	Area Of BW,At cm^2	Water Depth ds cm.	AVE. INC. Hmo cm	AVE. INC. Tp sec.	AVE. Trans. Hmo com	AVE. Kr	Cal. Hmo cm.	Structure Height as Built hc cm.	Damaged Structure Height hc cm.	Area Of Damage Ad cm^2
3	67	1	1.080	17	2.630	1560	25	10.420	1.430	4.610	0.242	9.740	29.140	24.110	119.660
3	68	1	1.100	17	2.630	1560	25	11.060	1.460	4.950	0.248	10.290	29.020	25.910	92.530
3	69	1	2.060	17	2.630	1560	25	8.430	2.250	4.110	0.410	8.310	29.440	26.610	66.430
3	70	1	3.060	17	2.630	1560	25	10.890	2.910	6.200	0.317	9.940	29.230	22.010	66.390
3	71	1	4.010	17	2.630	1560	25	2.590	3.590	0.920	0.600	2.550	28.860	28.100	15.140
5	72	1	1.100	17	2.630	2190	25	10.860	1.460	2.520	0.279	10.120	34.870	29.440	219.440
5	73	1	1.080	17	2.630	2190	25	9.380	1.450	1.680	0.272	8.830	34.380	32.190	113.160
5	74	1	1.070	17	2.630	2190	25	7.910	1.420	1.150	0.298	7.510	35.050	33.890	138.700
5	75	1	1.060	17	2.630	2190	25	7.520	1.460	0.990	0.289	7.150	34.780	34.560	83.430
5	76	1	1.040	17	2.630	2190	25	5.460	1.410	0.720	0.285	5.230	34.560	34.550	23.880
5	77	1	4.070	17	2.630	2190	25	15.720	3.580	7.690	0.322	12.220	34.780	20.120	644.190
5	78	1	1.070	17	2.630	2190	25	8.820	1.410	1.560	0.285	8.330	35.450	33.560	163.970
5	79	1	1.020	17	2.630	2190	25	2.750	1.440	0.570	0.354	2.650	35.270	35.260	3.900
5	80	1	2.100	17	2.630	2190	25	12.960	2.270	5.770	0.303	11.480	36.060	24.200	393.260
5	81	1	2.080	17	2.630	2190	25	10.890	2.280	4.320	0.335	10.340	35.170	26.610	345.970
5	82	1	2.060	17	2.630	2190	25	9.640	2.300	3.460	0.384	9.370	35.050	28.680	235.700
5	83	1	2.040	17	2.630	2190	25	6.790	2.300	1.440	0.489	6.790	35.270	33.590	116.690
5	84	1	2.020	17	2.630	2190	25	4.030	2.300	0.840	0.538	4.030	34.410	34.400	4.090
5	85	1	3.100	17	2.630	2190	25	15.340	3.000	7.230	0.312	11.910	34.990	21.610	514.590
5	86	1	3.080	17	2.630	2190	25	14.080	2.960	6.900	0.311	11.590	35.910	22.160	538.370
5	87	1	3.070	17	2.630	2190	25	12.750	2.860	6.320	0.314	11.040	35.540	23.040	429.580
5	88	1	3.060	17	2.630	2190	25	11.160	2.840	2.680	0.352	10.400	35.230	24.870	324.140
5	89	1	3.040	17	2.630	2190	25	7.580	2.850	2.680	0.477	7.310	35.140	29.720	184.970
5	90	1	3.020	17	2.630	2190	25	3.780	2.780	0.990	0.581	3.720	35.360	35.350	6.970
5	91	1	4.060	17	2.630	2190	25	14.290	3.560	6.890	0.364	11.710	35.170	21.030	555.190
5	92	1	4.040	17	2.630	2190	25	10.130	3.570	5.350	0.383	9.260	34.590	23.560	389.080
5	93	1	4.020	17	2.630	2190	25	5.330	3.560	2.320	0.524	5.190	34.810	27.010	231.330
5	94	1	4.010	17	2.630	2190	25	2.580	3.570	0.760	0.648	2.540	35.870	35.860	5.020
5	95	1	1.030	17	2.630	2190	25	4.280	1.440	0.650	0.341	4.110	35.570	35.420	8.360
5	96	1	1.050	17	2.630	2190	25	7.020	1.440	0.900	0.288	6.690	35.540	35.330	56.860
5	97	1	1.080	17	2.630	2190	25	9.990	1.330	1.980	0.290	9.370	35.170	31.760	187.200
5	98	1	1.100	17	2.630	2190	25	11.350	1.450	3.060	0.297	10.540	34.960	29.540	231.050
5	99	1	2.030	17	2.630	2190	25	5.480	2.290	1.030	0.509	5.470	35.480	34.440	51.560
5	100	1	2.060	17	2.630	2190	25	8.220	2.290	2.400	0.450	8.110	34.630	30.270	170.380
5	101	1	2.080	17	2.630	2190	25	11.030	2.280	4.410	0.363	10.440	35.300	27.340	293.850
5	102	1	2.050	17	2.630	2190	25	6.910	2.290	1.340	0.490	6.870	35.910	31.330	131.360
5	103	1	2.100	17	2.630	2190	25	13.020	2.280	6.070	0.318	11.500	35.080	24.050	329.250
5	104	1	3.010	17	2.630	2190	25	1.810	2.780	0.620	0.590	1.790	35.810	35.690	5.670
5	105	1	3.030	17	2.630	2190	25	5.680	2.810	1.590	0.521	5.550	35.750	31.760	146.600
5	106	1	3.050	17	2.630	2190	25	9.310	2.850	4.110	0.413	8.770	36.090	27.160	271.370
5	107	1	3.080	17	2.630	2190	25	13.870	2.860	6.500	0.357	11.520	35.630	22.190	502.700
5	108	1	3.100	17	2.630	2190	25	15.610	2.910	7.340	0.335	11.950	34.930	21.280	531.870
5	109	1	4.010	17	2.630	2190	25	2.560	3.560	0.780	0.624	2.520	35.910	35.900	2.690
5	110	1	4.030	17	2.630	2190	25	8.060	3.560	3.170	0.526	7.630	35.540	26.970	247.400
5	111	1	4.060	17	2.630	2190	25	14.460	3.540	7.330	0.335	11.780	35.360	20.360	588.170
5	112	1	4.070	17	2.630	2190	25	15.990	3.580	7.880	0.327	12.300	36.030	19.780	656.820
7	124	1	1.100	71	2.830	1900	25	11.440	1.450	3.910	0.354	10.610	31.460	31.210	42.460
7	125	1	1.080	71	2.830	1900	25	10.020	1.450	2.940	0.335	9.400	31.700	31.550	26.570
7	126	1	1.060	71	2.830	1900	25	8.030	1.440	2.000	0.352	7.620	31.360	31.350	20.070
7	127	1	1.040	71	2.830	1900	25	5.600	1.430	1.330	0.378	5.360	31.700	31.610	1.770
7	128	1	1.020	71	2.830	1900	25	2.600	1.430	0.820	0.430	2.500	31.670	31.660	3.530
7	129	1	2.100	71	2.830	1900	25	13.030	2.226	4.950	0.455	11.500	31.670	31.660	37.440
7	130	1	2.080	71	2.830	1900	25	11.110	2.300	4.060	0.471	10.500	32.340	31.970	18.950
7	131	1	2.060	71	2.830	1900	25	8.630	2.280	2.980	0.508	8.490	31.910	31.670	24.900
7	132	1	2.040	71	2.830	1900	25	5.580	2.280	1.720	0.537	5.570	32.060	31.730	9.660
7	133	1	2.020	71	2.830	1900	25	2.720	2.260	1.000	0.570	2.720	31.670	31.550	1.390

Subset NO.	Test NO.	Test Type	File And Gain	Median Weight W50 gr.	Density Of Stone wt.	Area Of BW,At cm^2	Water Depth ds cm.	AVE. INC. Hmo cm	AVE. INC. Tp sec.	AVE. Trans. Hmo com	AVE. Kr	Cal. Hmo cm.	Structure as Built hc cm.	Damaged Height Structure hc cm.	Area Of Damage Ad cm^2
7	134	1	3.100	71	2.830	1900	25	15.660	3.040	6.770	0.426	11.960	31.640	29.720	93.740
7	135	1	3.080	71	2.830	1900	25	14.030	2.880	6.120	0.409	11.580	32.160	29.750	106.840
7	136	1	3.060	71	2.830	1900	25	11.170	2.790	4.890	0.449	10.130	32.520	30.540	45.240
7	137	1	3.040	71	2.830	1900	25	7.420	2.820	2.850	0.502	7.160	31.670	31.540	7.900
7	138	1	3.020	71	2.830	1900	25	3.550	2.780	1.350	0.556	3.500	31.300	31.120	2.970
7	139	1	4.070	71	2.830	1900	25	15.860	3.580	8.010	0.409	12.260	31.390	24.320	258.360
7	140	1	4.060	71	2.830	1900	25	14.230	3.520	6.420	0.466	11.680	32.250	29.140	100.610
7	141	1	4.040	71	2.830	1900	25	10.380	3.550	4.490	0.511	9.440	31.390	30.210	50.450
7	142	1	4.020	71	2.830	1900	25	5.100	3.570	1.830	0.586	4.970	32.220	31.210	18.210
7	143	1	4.010	71	2.830	1900	25	2.350	3.600	0.980	0.596	2.320	31.670	31.660	9.010
7	144	1	1.030	71	2.830	1900	25	3.980	1.420	1.070	0.382	3.820	31.970	31.640	1.110
7	145	1	1.050	71	2.830	1900	25	6.740	1.390	1.590	0.356	6.430	31.850	31.790	3.160
7	146	1	1.080	71	2.830	1900	25	9.980	1.450	2.870	0.380	9.360	31.820	31.810	9.290
7	147	1	1.100	71	2.830	1900	25	11.420	1.450	3.620	0.379	10.590	32.000	31.730	23.230
7	148	1	2.030	71	2.830	1900	25	4.070	2.290	1.310	0.554	4.070	31.820	31.640	4.460
7	149	1	2.050	71	2.830	1900	25	7.070	2.290	2.340	0.526	7.030	31.610	31.460	5.330
7	150	1	2.090	71	2.830	1900	25	11.320	2.260	4.250	0.482	10.630	31.490	31.360	23.040
7	151	1	2.100	71	2.830	1900	25	13.110	2.230	5.100	0.461	11.530	31.610	30.510	40.880
7	152	1	3.010	71	2.830	1900	25	1.650	2.780	0.800	0.593	1.630	31.700	31.690	0.930
7	153	1	3.030	71	2.830	1900	25	5.660	2.790	2.020	0.554	5.540	31.820	31.030	20.250
7	154	1	3.050	71	2.830	1900	25	9.750	2.800	4.230	0.481	9.110	31.300	31.000	27.870
7	155	1	3.080	71	2.830	1900	25	14.240	2.810	6.040	0.423	11.650	31.240	29.630	56.300
7	156	1	3.100	71	2.830	1900	25	15.420	2.880	6.960	0.418	11.930	32.130	28.590	106.650
7	157	1	4.010	71	2.830	1900	25	2.350	3.580	1.000	0.588	2.320	32.800	32.770	1.300
7	158	1	4.030	71	2.830	1900	25	7.810	3.600	2.910	0.564	7.410	32.740	32.460	13.560
7	159	1	4.060	71	2.830	1900	25	14.510	3.550	6.840	0.452	11.800	32.220	26.970	146.420
7	160	1	4.070	71	2.830	1900	25	16.040	3.580	7.680	0.430	12.310	31.940	26.880	142.420
7	161	1	4.060	71	2.830	1900	25	14.420	3.540	6.680	0.471	11.760	31.860	28.250	129.510
9	188	1	4.040	71	2.830	1900	30	10.540	3.560	6.700	0.422	9.870	32.000	29.810	47.660
9	189	1	1.040	71	2.830	1900	30	5.760	1.430	3.140	0.256	5.520	31.820	31.790	8.550
9	190	1	1.080	71	2.830	1900	30	10.940	1.500	6.030	0.301	10.320	31.550	31.540	7.620
9	191	1	1.100	71	2.830	1900	30	12.630	1.500	6.950	0.285	11.800	31.730	31.240	7.840
9	192	1	2.040	71	2.830	1900	30	5.800	2.200	3.210	0.443	5.790	31.580	31.520	1.390
9	193	1	2.080	71	2.830	1900	30	12.020	2.190	7.130	0.388	11.620	31.670	31.060	17.280
9	194	1	2.100	71	2.830	1900	30	14.460	2.220	8.370	0.357	13.280	31.580	29.660	42.550
9	195	1	3.040	71	2.830	1900	30	8.200	2.990	5.090	0.436	7.960	32.000	31.760	7.250
9	196	1	3.080	71	2.830	1900	30	16.090	3.080	9.590	0.348	13.610	31.610	26.610	156.260
9	197	1	3.100	71	2.830	1900	30	18.170	3.060	10.330	0.344	14.250	32.060	25.510	191.290
9	198	1	4.020	71	2.830	1900	30	5.220	3.370	2.900	0.497	5.110	32.130	32.060	3.160
9	199	1	4.050	71	2.830	1900	30	13.380	3.310	8.380	0.405	11.970	32.000	28.640	99.310
9	200	1	4.070	71	2.830	1900	30	17.600	3.280	10.470	0.362	14.230	31.610	25.210	198.630
2	12	2	2.040	17	2.630	1170	25	5.870	2.240	4.170	0.321	5.860	19.990	19.991	1.770
2	19	2	2.040	17	2.630	1170	25	5.870	2.230	4.610	0.271	5.860	19.100	16.860	1.580
2	24	2	2.040	17	2.630	1170	25	5.950	2.230	4.690	0.243	5.930	15.880	15.910	0.650
4	55	2	2.040	17	2.630	1560	25	5.510	2.260	3.930	0.215	5.500	19.450	19.390	2.420
4	57	2	2.020	17	2.630	1560	25	2.720	2.240	2.120	0.180	2.720	18.010	17.980	1.020
4	58	2	2.040	17	2.630	1560	25	5.450	2.220	4.210	0.210	5.440	17.980	17.830	0.740
4	59	2	2.060	17	2.630	1560	25	8.350	2.230	6.030	0.228	8.230	17.830	17.800	0.560
4	60	2	2.080	17	2.630	1560	25	11.180	2.230	7.330	0.261	10.540	17.800	17.860	-0.650
4	61	2	2.100	17	2.630	1560	25	13.270	2.230	8.040	0.272	11.580	17.860	18.010	0.190
4	62	2	1.020	17	2.630	1560	25	3.170	1.440	2.120	0.125	3.050	18.010	17.890	1.490
4	63	2	1.040	17	2.630	1560	25	5.560	1.440	3.980	0.150	5.320	17.890	17.740	0.840
4	64	2	1.060	17	2.630	1560	25	7.990	1.440	5.220	0.178	7.580	17.740	17.680	0.190
4	65	2	1.080	17	2.630	1560	25	9.920	1.440	6.110	0.213	9.310	17.680	17.560	0.460
4	66	2	1.100	17	2.630	1560	25	11.190	1.460	6.680	0.229	10.400	17.560	17.710	-1.110
6	113	2	1.020	17	2.630	2190	25	2.840	1.430	2.010	0.151	2.730	19.780	19.810	-0.840

A5

Subset NO.	Test NO.	Test Type	File And Gain	Median Weight W50 gr.	Density Df Stone wt.	Area Df BW,At cm^2	Water Depth ds cm.	AVE. INC. Hmo cm	AVE. INC. Tp sec.	AVE. Trans. Hmo com	AVE. Kr	Cal. Hmo cm.	Structure Height as Built hc cm.	Damaged Structure Height hc cm.	Area Df Damage Ad cm^2
6	114	2	1.070	17	2.630	2190	25	9.040	1.430	4.870	0.214	8.530	19.810	19.600	4.370
6	115	2	1.040	17	2.630	2190	25	5.590	1.400	3.500	0.159	5.350	19.600	19.630	0.370
6	116	2	1.060	17	2.630	2190	25	8.120	1.440	4.510	0.201	7.700	19.630	19.540	2.140
6	117	2	1.080	17	2.630	2190	25	9.980	1.440	5.240	0.235	9.360	19.540	19.630	NA
6	118	2	1.100	17	2.630	2190	25	11.470	1.450	5.680	0.245	10.640	19.630	19.960	4.740
6	119	2	2.020	17	2.630	2190	25	2.490	2.220	1.840	0.185	2.490	19.960	19.780	0.370
6	120	2	2.040	17	2.630	2190	25	5.180	2.230	3.660	0.180	5.170	19.780	19.810	1.300
6	121	2	2.060	17	2.630	2190	25	7.960	2.220	4.990	0.206	7.870	19.810	19.811	1.490
6	122	2	2.080	17	2.630	2190	25	10.660	2.250	6.100	0.233	10.180	19.810	19.960	3.440
6	123	2	2.100	17	2.630	2190	25	12.880	2.230	6.690	0.260	11.450	19.960	19.750	3.160
8	162	2	1.010	71	2.830	1900	25	1.090	1.430	0.570	0.351	1.050	28.250	28.380	1.580
8	163	2	1.020	71	2.830	1900	25	2.430	1.430	0.960	0.284	2.340	28.380	28.190	0.560
8	164	2	1.030	71	2.830	1900	25	3.990	1.440	1.420	0.247	3.830	28.190	28.250	NA
8	165	2	1.040	71	2.830	1900	25	5.380	1.440	1.910	0.238	5.150	28.250	28.220	0.560
8	166	2	1.060	71	2.830	1900	25	7.800	1.450	2.770	0.249	7.410	28.220	28.190	1.760
8	167	2	1.080	71	2.830	1900	25	9.780	1.460	3.740	0.272	9.190	28.190	28.350	1.110
8	168	2	1.100	71	2.830	1900	25	11.030	1.450	4.360	0.299	10.270	28.350	28.180	1.670
8	169	2	2.010	71	2.830	1900	25	1.160	2.280	0.700	0.483	1.160	28.160	28.161	1.760
8	170	2	2.020	71	2.830	1900	25	2.550	2.270	1.190	0.454	2.550	28.160	28.250	0.650
8	171	2	2.030	71	2.830	1900	25	3.940	2.260	1.760	0.437	3.940	28.250	28.190	0.460
8	172	2	2.040	71	2.830	1900	25	5.440	2.300	2.500	0.436	5.430	28.190	28.220	1.670
8	173	2	2.060	71	2.830	1900	25	8.730	2.260	3.980	0.408	8.580	28.220	28.221	1.110
8	174	2	2.080	71	2.830	1900	25	11.260	2.280	5.150	0.395	10.600	28.220	28.290	0.190
8	175	2	2.100	71	2.830	1900	25	13.310	2.240	6.320	0.391	11.590	28.290	27.650	6.040
8	176	2	3.010	71	2.830	1900	25	1.620	2.780	0.920	0.493	1.600	27.650	27.610	0.650
8	177	2	3.020	71	2.830	1900	25	3.550	2.800	1.630	0.463	3.500	27.610	27.580	-0.650
8	178	2	3.030	71	2.830	1900	25	5.600	2.800	2.630	0.440	5.480	27.580	27.610	1.110
8	179	2	3.040	71	2.830	1900	25	7.590	2.830	3.810	0.400	7.310	27.610	27.650	3.160
8	180	2	3.060	71	2.830	1900	25	11.340	2.840	5.460	0.393	10.240	27.650	27.651	2.040
8	181	2	3.080	71	2.830	1900	25	14.160	2.800	6.680	0.391	11.620	27.650	28.010	0.370
8	182	2	3.100	71	2.830	1900	25	13.320	1.800	5.950	0.350	11.160	28.010	27.550	2.600
8	183	2	4.010	71	2.830	1900	25	2.250	3.580	1.130	0.515	2.220	27.550	28.010	0.370
8	184	2	4.020	71	2.830	1900	25	5.010	3.590	2.510	0.493	4.880	28.010	27.580	2.420
8	185	2	4.030	71	2.830	1900	25	7.500	3.560	3.940	0.474	7.150	27.580	27.680	1.110
8	186	2	4.040	71	2.830	1900	25	9.930	3.540	5.120	0.457	9.120	27.680	27.580	3.810
8	187	2	4.050	71	2.830	1900	25	12.260	3.540	6.040	0.445	10.680	27.580	27.490	2.600
10	201	2	2.020	71	2.830	1900	30	2.580	2.210	2.270	0.295	2.580	25.210	25.211	1.860
10	202	2	2.040	71	2.830	1900	30	5.570	2.220	4.310	0.290	5.560	25.210	25.180	2.230
10	203	2	2.060	71	2.830	1900	30	9.750	2.220	6.330	0.286	8.690	25.180	25.120	0.056
10	204	2	2.080	71	2.830	1900	30	12.250	2.220	8.000	0.299	11.800	25.120	24.960	2.970
10	205	2	2.100	71	2.830	1900	30	14.410	2.220	8.920	0.306	13.260	24.960	25.020	2.230

APPENDIX B: REGRESSION ANALYSIS USED TO DEVELOP FIGURE 29
SHOWING ENERGY DISTRIBUTION IN VICINITY OF REEF

1. For the energy dissipation figure (Figure 29) the following equation was used to predict the wave transmission coefficient:

$$K_t = \frac{1.0}{1.0 + C_1 \left(\dfrac{h_c}{d_s}\right)^{C_2} \left(B_n\right)^{C_3}}$$

where

$C_1 = 0.02945$

$C_2 = 3.329$

$C_1 = 0.585$

$R^2 = 0.859$

$F = 611$

2. The wave reflection curves shown in Figure 29 were calculated using the following equation:

$$K_r = \exp\left[C_1 \left(\frac{h_c}{d_s}\right) + C_2 \left(\frac{d_s}{h_c}\right) + C_3 \left(\frac{d_s}{L_p}\right)\right]$$

where

$C_1 = 0.2899$

$C_2 = -0.7628$

$C_3 = -7.3125$

$R^2 = 0.984$

$F = 4,175$

APPENDIX C: NOTATION

A_d Area of damage (cm^2)

A_t Cross-sectional area of breakwater (cm^2)

B_n Bulk number, defined by Equation 3

C Response slope of reef to wave action, defined by Equation 5

C' Effective "as built" reef slope, defined by Equation 4

C_1 Dimensionless coefficient

d_s Water depth at toe of breakwater (cm)

d_{50} $(W_{50}/w_r)^{1/3}$, typical dimension of the median stone (cm)

F $h_c - d_s$, freeboard of structure which for reef can be either positive or negative (cm)

h_c Crest height of breakwater after wave attack (cm)

h_c' Crest height of breakwater "as built" (cm)

H_c Zero-moment wave height at transmitted gage locations with no breakwater in channel (cm)

H_t Zero-moment transmitted wave height (cm)

H_{mo} Incident zero-moment wave height (cm)

K_r Reflection coefficient of breakwater as defined and calculated by method of Goda and Suzuki (1976)

K_t H_t/H_c , wave transmission coefficient

L_p Airy wave length calculated using T_p and d_s (cm)

N_s Stability number, defined by Equation 1

N_s^* Spectral stability number, defined by Equation 2

T_p Wave period of peak energy density of spectrum (sec)

w_r Density of stone (g/cm^3)

w_w Density of water, tests conducted in fresh water, $w_w = 1.0$ (g/cm^3)

W_{50} Median stone weight (subscript indicates percent of total weight of gradation contributed by stones of lesser weight) (g)